Cloning and characterization of glycolytic pathway enzymes from *Caldicellulosiruptor saccharolyticus*

WAGENINGEN UNIVERSITY
WAGENINGEN UR

Cloning and characterization of the glycolytic pathway enzymes from *Caldicellulosiruptor saccharolyticus*

Wageningen, 2011

Master Thesis
July ’10 - March ‘11

Supervisor
Bram Bielen

Student
Erik Sebus

Examinator
Servé Kengen

WAGENINGEN UNIVERSITY
WAGENINGEN UR

1 Voorwoord

Dit is het op een na laatste maar grootste product van mijn master studie biotechnologie in Wageningen. Nu ik bijna klaar ben met mijn studie, vind ik dat ik kan terug kijken op een geweldige en erg leuke periode hier in Wageningen. Ik heb biotechnologie altijd aantrekkelijk gevonden vanwege haar directe toepassing voor onze maatschappij. Dat is precies waarom ik deze scriptie heb gekozen, waarmee waterstof productie uit biomassa verbeterd kan worden.

Werken aan deze thesis zou een heel stuk zwaarder zijn geweest als ik niet zo veel mensen had gehad die me motiveerde of met wie ik ´gewoon´ een koffie praatje had. Daarom wil ik de volgende mensen bedanken:
Ten eerste, Bram Bielen voor zijn begeleiding en suggesties, maar vooral voor de ruimte die ik kreeg om aan de organisatie van een career event te werken én om een functie als bestuurslid van mijn studie vereniging uit te voeren, beide tijdens deze scriptie. Dit heeft een flexibele instelling vereist. Verder bedank ik ook Servé Kengen, voor zijn input in dit werk. Uiteraard ook alle mensen op het lab van microbiologie, bedankt voor jullie behulpzaamheid en warme welkom. Mede studenten bedankt voor jullie gezelligheid, ik zal de overmatige hoeveelheid koffie praat niet vergeten. Marieke wil ik bedanken voor alle lange en korte (motivatie) praatjes. Natuurlijk hoop ik niemand te zijn vergeten, maar anders, sorry en alsnog bedankt.

Als laatste wil ik mijn ouders bedanken voor hun motivatie en steun om überhaupt te beginnen aan deze studie, en voor een aantal financiële reddingsacties. Natuurlijk vergeet ik Lydia niet. Ondanks dat je er niet zo op gesteld was dat ik naar Wageningen ging, liet je me alles doen waar ik zo druk mee ben geweest. Bedankt voor je geduld en steun!

Erik Sebus
Maart 2011

2 Preface

This is the penultimate and largest product of my master study biotechnology in Wageningen. Now that I am close to finishing this study, I feel that I can look back at a great and very fun period here in Wageningen. I always thought that one of the major benefits of biotechnology was its applicability into today's society. Which is exactly why I chose this thesis subject, which could improve hydrogen production on a biomass basis.

Working on this thesis would have been a whole lot more bothersome if it wasn't for all the people who encouraged and motivated me or with whom I 'simply' had a nice coffee chat. Therefore I would like to thank the following people:
First, Bram Bielen for his supervision and suggestions, but above all for giving me room to work on the organization of a career event ánd to be active in the board of my study association both during this thesis. This has required a flexible set of mind. I also thank Servé Kengen for his input in this work. Of course all the people on the lab of microbiology, thank you for your assistance and warm welcome. Also my co-students thank you all for all the fun, I will not forget the abundant coffee talks. I would like to thank Marieke for all the big and small (motivation) talks. Of course I hope I didn't forget anyone, if so, sorry and thanks!

Finally I would like to thank my parents for their motivation and support to actually start this study, and performing several financial rescues. Thanks! Of course I will not forget Lydia. Even though you weren't very fond of me going to Wageningen, you let me do all the things that kept me so busy. Thank you for your patience en support!

Erik Sebus
March 2011

3 Abstract

At some point fossil fuel will be depleted and alternative energy sources need to be explored. One promising alternative is bio-hydrogen. A very good hydrogen producer is *Caldicellulosiruptor saccharolyticus*, which can produce hydrogen close to the theoretical maximum of 4 mol/mol hexose (3.6 mol/mol hexose). In addition to a PK and a ATP-PFK, a PPDK and a PPI-PFK are present. The activation of these additional enzymes is interesting since they increase the ATP yield on glucose. However it is not known if and what regulation is taking place. The genes for these four enzymes were cloned to an *E.coli* BL21de3 strain, produced and purified. This resulted in quite pure enzymes. So far the two regular enzymes, the ATP-PFK and the PK have been shown to be active under enzyme essay conditions. From here these enzymes can be subjected to characterization studies in order to unravel the potential regulation method. These insights might make it possible to increase the flux through these rare enzymes, increasing the ATP yield on glucose and as such the biomass/glucose yield.

Table of content

4 Introduction

4.1 General introduction to research topic

Currently we are burning through our fossil fuels reserves (Shafiee and Topal 2009). Although predictions may differ from each other, it is obvious that we will run out of fossil fuels sooner or later since it takes several million years to build the reserves we burned in a few decades. Since a major part of our society heavily relies on fossil fuels, alternative energy sources will need to be investigated.

Fortunately, multiple possibilities are already being investigated. A few of these new energy sources are for example, wind energy, geothermal power, municipal waste to energy programs, tidal power, solar power and biomass. However, solar and wind energy require a large area and are not available everywhere, neither is geothermal power. It is likely that none of these solutions will be the sole solution. Rather a combination of these solutions will be the answer to our imminent energy crisis (Fridleifsson 2003)

Biomass can be used in various ways to produce energy. Biodiesel, bio-ethanol and gasification (Rajvanshi 1986) and biological hydrogen production by micro-organisms are examples of this. Currently all of these application are being developed and improved (Rostrup-Nielsen 2005). This thesis focuses on a hydrogen producing organism.

Hydrogen has a very high chemical energy. When comparing on a mass to mass basis, hydrogen has three times more energy compared to other chemical fuels (Schlapbach and Zuttel 2001). This makes hydrogen a promising fuel.

4.2 Caldicellulosiruptor saccharolyticus

Hydrogen production by micro-organisms from renewable biomass is preferred since this enables a CO_2 neutral production. For this production, the use of thermophilic bacteria is more favorable than mesophilic bacteria. The reason for this is because under thermophilic conditions, less reduced metabolic end products are formed that compete with the hydrogen production (Claassen 2006). This is because at higher temperatures the production of hydrogen from NADH and ferredoxin is more favorable, compared to the production at lower temperatures. At lower temperatures more NADH and ferredoxin is therefore recycled into other reduced end products and results in a lower theoretical maximum. A particularly good hydrogen producer is *Caldicellulosiruptor saccharolyticus* with a production yield of 3,6 mole (de Vrije, Mars et al. 2007), which can be even further increased to nearly 9 mole, of hydrogen per mole of glucose (Claassen 2006).

Caldicellulosiruptor saccharolyticus was isolated from a geothermal spring in Taupo, New Zealand in 1987 by Sissons and coworkers (Sissons,

Sharrock et al. 1987). Characterization of this organism was carried out in 1994 by Rainey et all. The literal meaning of *Caldicellulosiruptor* is: "breaker of hot cellulose", whereas *saccharolyticus* refers to the ability to degrade polysaccharides (Rainey, Donnison et al. 1994). *C. saccharolyticus* is an extreme thermophilic (opt. temp. 70 °C) strictly anaerobic gram-positive bacterium (Rainey, Donnison et al. 1994) and produces hydrogen, acetate, lactate, and traces of ethanol from a broad range of sugars (Rainey, Donnison et al. 1994). Production of hydrogen is inhibited by 27,7 mM (pH_2 of $5.6*10^4$ Pa) in the gas phase (van Niel, Claassen et al. 2003). A metabolic shift to lactate production will occur at 5–10 mM H_2 (1 á 2 * 10^4 Pa) in the gas phase.

4.3 Zooming in: the enzymes

Using NMR analysis of C^{13} labelling patterns it has become clear that the main glycolytic route is the Embden-Meyerhof pathway (de Vrije, Mars et al. 2007). Furthermore this organism genome was sequenced in 2008 (van de Werken, Verhaart et al. 2008). The annotated genome sequence revealed that in addition to the regular PK and ATP PFK this organism has an PPDK and PPi PFK, see figure 4.1.

Especially the PK and PPDK are interesting because the use of PPDK yields an extra ATP in comparison to the PK. Characterization studies on PPDK mostly involve aromatic compounds (BRENDA 2011). At this moment it is not exactly known whether or not the activity of PK and PPDK is regulated. However, results indicating that PK is inhibited by PPi are observed with characterization on cell free extract (Bielen, Willquist et al. 2010). Despite the fact that the PK and PPDK are clustered on different parts of the genome, they seem to be up-regulated under the same conditions (van de Werken, Verhaart et al. 2008).

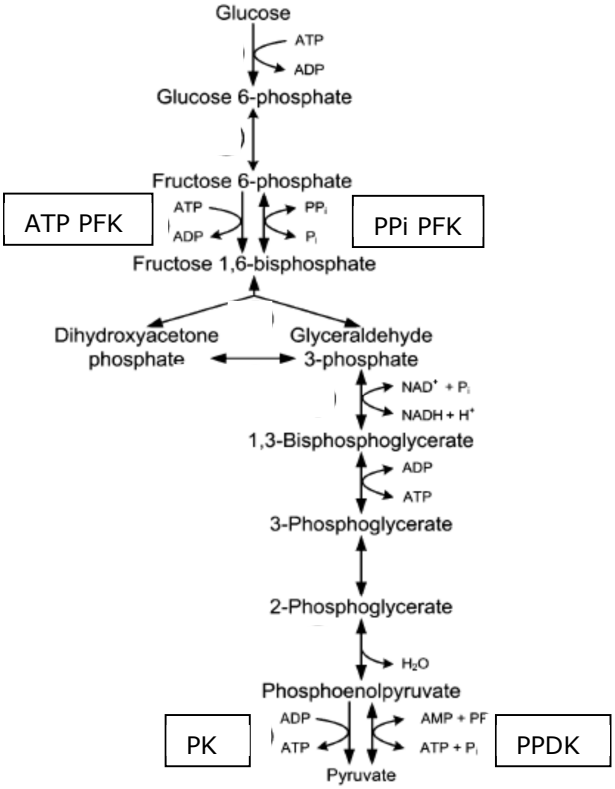

Figure 4-1 Main glycolytic pathway in Caldicellulosiruptor saccharolyticus, the Embden Meyerhof pathway. Adapted from (Bielen, Willquist et al. 2010)

ATP dependent phosphofructo kinase (EC. 2.7.1.11) catalyses the reaction ATP + D-fructose 6-phosphate = ADP + D-fructose 1,6-bisphosphate. This is the first irreversible reaction of the glycolysis. The enzyme is regulated by the ATP/AMP ratio. Since high ATP levels inhibit and AMP activates the enzyme, the glycolysis is regulated by intracellular energy levels(Lindell and Stellwagen 1968). Some Km values that are known are, ATP 0.005-0.7 mM, ADP 0.5-1.4 mM, fructose 1,6 bisphosphate 7.6-16 mM and fructose 6-phosphate 0.011-7 mM. ATP PFK has been found as a dimer (*Escherichia coli*) a hexamer, octamer (*Saccharomyces cerevisiae*), but mostly as a tetramer (*Thermotoga maritima, Escherichia coli, Clostridium pasteurianum*) (Uyeda and Kurooka 1970; Kotlarz and Buc 1981; Ding, Ronimus et al. 2001; Bárcena, Radermacher et al. 2007; BRENDA 2011).

In addition to the ATP PFK, the PPi dependent phosphofructo kinase (EC. 2.7.1.90) catalyses the reaction diphosphate + D-fructose 6-phosphate = phosphate + D-fructose 1,6-bisphosphate. It has been proposed that this enzyme is the anaerobic equivalent of the ATP PFK, as the use of PPi instead of ATP would potentially increase the ATP yield on glucose (Mertens 1991). Because PPi is only abundantly available during exponential growth it is highly likely that this enzyme is co-existent with ATP PFK and the enzymes are actively regulated. However little is known about PPi PFK regulation, as regulators of ATP PFK do not effect PPi PFK (Siebers, Klenk et al. 1998; BRENDA 2011). Km values are known and some ranges are given: fructose 1,6-bisphosphate 0.08-0.32 mM, fructose 6-phosphate 0.03-2.3 mM and PPi 0.01-0.6 mM. This enzyme exists in monomer and octamer, but the main forms are the dimer (*Toxoplasma gondii, Propionibacterium freudenreichii subsp. shermanii*) and tetramer (*Thermoproteus tenax, Daucus carota*)(O'Brien, Bowien et al. 1975; Peng and Mansour 1992).

Pyruvate kinase (EC. 2.7.1.40) produces pyruvate according to the following reaction ATP + pyruvate = ADP + phosphoenolpyruvate (PEP). PK is present in the classical Embden Meyerhof pathway. Some Km values for this enzyme are, ADP 0.8-1.5 mM and PEP 0.02-2.1 mM. This enzyme is mostly found as a tetramer (*Thermotoga maritima, Saccharomyces cerevisiae, Homo sapiens*) (Aust and Suelter 1978; Johnsen, Hansen et al. 2003; Pendergrass, Williams et al. 2006).

PPDK (EC. 2.7.9.1) is found in bacteria, archaea and plants. However, most of the characterization is performed on parasitic protozoan and plants. The enzyme catalyses the reaction ATP + pyruvate + phosphate = AMP + phosphoenolpyruvate + diphosphate. Km values for substrates range from, AMP 0.001-0.02mM, ATP 0.004-8 mM, diphosphate 0.029-0.1 mM, phosphate 0.0014-1.8 mM, PEP 0.02-0.5 mM and pyruvate 0.025-0.8 mM. The known structures of this organism are primarily a dimer (*Clostridium symbiosum*) and a tetramer (*Zea mays, Entamoeba histolytica*) (Sugiyama 1973; Saavedra, Encalada et al. 2005)

4.4 The aim

This thesis aims to unravel the regulation of the enzymes: ATP PFK, PPi PFK, PK and PPDK from *C. saccharolyticus*. To that end, genes encoding these enzymes were individually cloned into an (inducible) plasmid, which were used to transform an *E.coli* expression strain. Enzymes were produced and purified. The purified enzymes will be used for characterization assays.

4.5 Outline of the project

In figure 4.2 the flow of the project is shown.

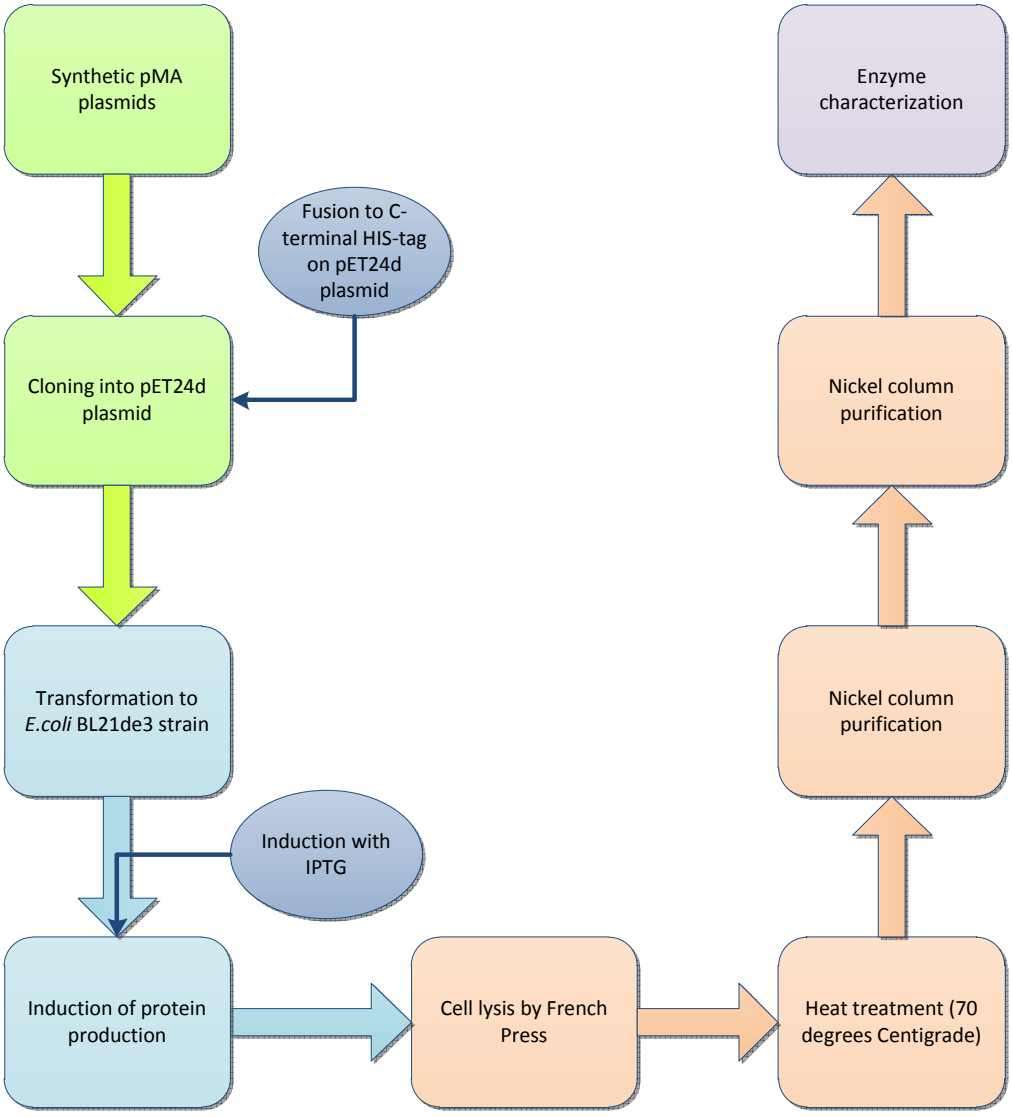

Figure 4-2 Outline of the project. Synthetic plasmids with codon optimized for *E.coli* genes from *C.saccharolyticus* are already ordered. These genes will be inserted into an inducible pET24d plasmid. The production strain, *E.coli* BL21de3 will be grown and protein production will be induced. In several steps, the protein will be purified. After the nickel column a desalting step will take place and the proteins will be analyzed for multimerity on a superdex and a purity check on SDS page (these steps are not shown in the diagram). Finally the enzymes will be characterized.

5 Material and Methods

5.1 Media

LB medium consisted of 10 g/l NaCl, 10 g/l triptone and 5 g/l yeast extract. Agar plates were made by adding 15 gram of agar granules per liter LB medium before sterilization. Optional 50 µg/ml of antibiotics were added to the medium or agar to create selection medium or selection plates. SOC medium contained per liter, triptone 20.0 g, yeast extract 5.0 g, sodium chloride 0.5 g, magnesium sulfate (anhydrous) 2.4 g and potassium chloride 186.0 mg. After sterilization 20 ml 20% (w/v) of glucose was added by filter sterilization.

5.2 Storage of genetic material and cultures

All genetic material: primers, plasmids, vectors and constructs, were stored at -20°C in MilliQ. *E.coli* DH5α and *E.coli* BL21de3 strains were stored in 30% glycerol at -80°C.

5.3 Gene cloning

5.3.1 Carrier plasmid and destination vector propagation

Four synthetic plasmids (pMA) containing the genes Csac_1830 (ATP PFK), Csac_1831 (PK), Csac_1955 (PPDK) and Csac_2366 (PPi PFK) respectively, were purchased from GeneArt. The *C. saccharolyticus* genes were codon optimized for *E.coli*. A pET24d plasmid was used as destination vector. This plasmid contained a His-tag and a stop codon in frame with insert, see appendix 11.2, 11.3 and 11.4 for more information. The pMA plasmids and the pET24d plasmid were transformed to individual *E.coli* DH5α cells (competent cell appendix 11.11.1) and incubated at 37°C for 45-60 minutes with LB medium. 100 µl of culture was plated on a selection plate (50 µg/ml ampicillin) and incubated overnight (37 °C). The plates were then stored at 4 °C.

5.3.2 Plasmid isolation

Colonies were picked from agar selection plates and grown overnight (37°C) in 10 ml LB with selection maker (50 µg/ml). For the pET24d destination vector 50 µg/ml of kanamycin, and for the pMA plasmids 50 µg/ml ampicillin was used. The culture was spun down and the plasmids were isolated using the Fermentas miniprep kit.

5.3.3 Plasmid and vector restriction

Subsequent restriction was performed in REact2 buffer (Invitrogen) using the following enzymes: NcoI (Fermentas) and XhoI (Invitrogen) for pET24d, pMA_Csac1830 and pMA_Csac2366, BsphI (NEB) and XhoI were used to digest pMA_Csac1831 and pMA_Csac1955. The total volume was 20 µl containing 1 µl of each restriction enzyme and 2 µl of buffer REact 2

(10x). Total incubation time was 2.5 h at 37°C. After 1.5 hour of incubation Antarctic Phosphatase and Antarctic Phosphatase buffer was added to the pET24d restriction.

5.3.4 Restriction fragment separation and isolation

After restriction, the pET24d vector was desalted using the Zymo DNA clean and concentrator kit and was eluted in 20 µl MilliQ. The pMA fragments were loaded in a 1% agarose gel and placed in a gel electrophoreses apparatus (Anachem Mupid one). During 45-60 minutes, 100V was applied to the gel which caused the DNA fragments to migrate through the gel according to size. With the Bio-Rad UV Transilluminator the DNA bands were visualized and fragments with a size equal to the specific Csac_gene were cut from the gel. With a QIAEX gel extraction kit the DNA was isolated from the gel.

5.3.5 Ligation

The pET24d (destination vector) and the pMA fragment (respective Csac_gene) were mixed in a 1:3 ratio (vector: insert) and T4 ligase and T4 ligase buffer was added. As a background measurement an open vector was mixed with water T4 ligase and T4 ligation buffer. These mixtures were incubated 10 minutes at 20° centigrade.

5.4 Transformation

5.4.1 Heat shock transformation

2 µl of the ligation mix was added to 25 µl commercial heat shock competent *E.coli* DH5α cells (NEB 5-alpha Competent *E. coli* (High Efficiency) C2987H). As a background measure, ligation mix only containing the restriction product from pET24d was added to the competent cells. The background measure was used to estimate the number of positive colonies on the plate, because the colonies of the background indicate self-ligation of the pET24d vector. After 45-60 minutes of recovery (37°C) on SOC medium, 100 µl culture was plated on LB plates containing 50 µg/ml kanamycin. The plates were incubated overnight in an incubation stove at 37°C.

5.5 Analysis of pET24d_(Csac_gene) construct

5.5.1 Colony PCR

A colony PCR was performed on a sensible amount of colonies, usually three times the background (background measure 5.3.5). T7 forward and reverse primers were used. These primers both start on the pET24d vector and elongate their product over the insert. The PCR mixture contained 0.1 µM forward and reverse primer, 200 µM dNTP's 0.05 unit/µl REDTaq DNA polymerase and 1x REDTaq PCR Reaction buffer. With milliQ, the volume was increased to 20 µl. The PCR machine program was: first 10 min 95^{o}C for destroying the cell walls, then 30 repeats of 30 sec 95^{0}C

(denaturing), 30 sec 50°C (annealing) and 180 sec 72°C (elongation). After the repeats the machine was hold up at 4°C. The resulting products were placed on a 1% agarose gel together with a 1kb DNA ladder from Fermentas (appendix 11.1) to estimate if the products have the proper size.

5.5.2 Restriction analysis of construct

In addition to the colony PCR, the restriction pattern of the same colonies was analyzed. For this the colonies were cultivated overnight in LB medium with kanamycin (50 µg/ml) and the plasmids were isolated using the Fermentas miniprep kit. Restriction enzymes, XhoI (Invitrogen) and EcoRV (Invitrogen) for pET24d_1830, pET24d_1831 and pET24d_1955 for pET24d_2366 NcoI (Fermentas) and XhoI (Invitrogen), were added and the resulting pattern was analyzed on agarose gel.

5.5.3 Sequencing

Based on the results from the construct analysis samples were sent for sequence analysis before experiments were continued. 750 ng of DNA in less than 20 µl was sent to BaseClear.

5.6 Transformation to production strain

Constructs (pET24d_1830 pET24d_1831 pET24d_1955 pET24d_2366) that were considered positive were transformed to *E.coli* BL21de3 cells by means of electro shock, see appendix 11.11.2.

5.7 Protein expression

BL21de3 transformants were grown overnight in 5 ml LB medium containing 50 µg/ml kanamycin at 37°C. 1 ml of culture was used to inoculate 1 L of LB (50 µg/ml kanamycin) and incubated at 37°C. When the culture reached an OD of ~2.0 the cells were induced with 0.1 mM IPTG (appendix 11.11.3). The culture was incubated overnight at 37°C.

5.8 Protein harvest

The induced cells were spun down using a RC6 sorvall centrifuge with SLA3000 rotor at 10,000 rpm for 15 minutes at 4°C. The cell pellet was dissolved in 30 ml of 300 mM NaCl, 10 mM imidazole, 50 mM Tris/HCl pH 7.5. The resuspended cells were disrupted by passing the suspension through a French press twice. A small amount of DNAseI was added to the disrupted cells, and kept at room temperature for 15 minutes in order to destroy the DNA. The cell debris was spun down in a RC6 sorvall centrifuge with SS34 rotor at 16,000 rpm for 15 minutes at 4°C and the cell free extract (CFE) was obtained. CFE and pellet were stored at 4°C.

5.9 Protein purification

5.9.1 Heat treatment

The 15 ml CFE was incubated at 70°C for 20 minutes. The denatured protein was then spun down with a RC6 sorvall centrifuge with a SS34 rotor for 15 minutes at 16,000 rpm at 4°C and heat stable cell free extract (HSCFE) was obtained. HSCFE and Hpellet were stored at 4°C (more on heat treatment, appendix 11.11.4).

5.9.2 Ni column purification

In order to purify the protein a nickel column, HisPrep^{tm} FF 16/10 (see appendix 11.5), and Äkta FPLC system operated by the Unicorn 5.1 software was used. The maximum pressure was set at 0.3 Mpa and a flow of 3ml/min was used, a 20 ml loop was installed. The HSCFE (15 ml) was filtered on a 0.2 µM filter and loaded in the loop. Using buffer A, 300 mM NaCl, 50 mM Tris/HCl pH 7.5, the loop was loaded on the column. The loop was flushed with 10 ml buffer A and the column was washed with 4 column volumes (CV). The gradient delay was set at 20 ml and the gradient was spread over 8 CV. At the end of the gradient 100% of buffer B, 300 mM NaCl, 500mM imidazole, 50 mM Tris/HCl pH 7.5, flushed though the system. An increasing salt gradient (imidazole) will displace the proteins bound to the nickel column, these proteins are collected in fractions of 4 ml.

5.9.3 Desalting

Selected fractions were desalted, using a HisPrep Desalting 26/10 column (see appendix 11.6) and a 50mM Tris/HCl buffer at pH 7.5 as an eluent. The FPLC was operated manually starting fractionation when protein started washing off the column. The maximum pressure was at 0.85 Mpa.

5.9.4 Superdex analysis

Purified protein samples were run over a Superdex™ 200 Column (see appendix 11.6) on the Äkta FPLC system operated by the Unicorn 5.1 software, in order to estimate the undenatured protein size. Calibration mixtures were prepared: Blue Dextran (1mg/ml) to estimate the void volume; ribonuclease A, ovalbumin, aldolase and ferritin were mixed for Run I and chymotrypsinogen A, albumin and catalase were mixed as Run II. From the calibration mixtures 250 µl was loaded. A buffer solution of 50 mM Tris/HCl pH7.5, 150mM NaCl was used as a running liquid (1ml/min). 250 µl of sample was loaded on the column and slowly eluted from the column.

5.9.5 SDS page

SDS (running) gels were made in pairs of two (10ml total) and contained: 4.0 ml H_2O, 3.3 ml 30% acrylamide mix. 2.5 ml 1.5 M Tris/HCl pH 8.8, 0.1 ml 10% SDS, 0.1 ml ammonium persulfate. Polymerization was induced by adding 4 µl TEMED. During polymerization the gel was separated from air by propanediol. Stacking gels were made and added after the running

gel had polymerized (~30min) and contained: 1.4 ml H2O, 0.33 ml 30% acrylamide mix, 0.25 1.5 M Tris/HCl pH 6.8, 0.02 ml 10% SDS, 0.02 ml ammonium persulfate. Polymerization was started by adding 3 µl TEMED. A comb was placed (20 µl) in order to form the slots and the air bubbles were carefully removed. Technical details on SDS page can be found in appendix 11.11.5.
Samples were pre-treated by mixing with loading buffer (50 mM Tris/HCl pH 6.8, 100 mM DTT, 2% SDS, 0.1% bromophenol blue and 10% glycerol) and incubate for 3 minutes at 95°C. A 250 kDa marker from Bio-Rad was used, see appendix 11.1. As for the settings for running the gel, 20V per gel was applied for 60 minutes.
Protein samples (10 µl) from different stages of purification were run on a SDS page gel, a protein marker (appendix 11.1) was run along with the samples in order to estimate the protein size.

5.10 Total protein determination

The Roti®-Nanoquant method (Roth) was used to determine total protein concentrations. A working solution of Roti®-Nanoquant reagents at a 1x concentration and a BSA calibration series of 1, 10, 20, 40, 60, 80 and 100 µg/ml was prepared. First the machine was zeroed against water. The samples were diluted 1:20 and a 1:40. From the samples and the calibration series 200 µl was mixed by inversion with 800 µl Roti®-Nanoquant reagents 1x. This was measured at 590 nm and 450 nm. The quotient (590/450) was plotted in a graph and used for concentration calculations.

5.11 Enzyme assays

5.11.1 pH variations

The activity of the pyruvate kinase was measured at different pH (70°C) values (6.0, 6.5, 7.0, 7.5). The temperature effect (dpK_a/dT=-0.028) was taken into account when adjusting the pH of the buffer. Activity was determined at these pH values and the best performing condition was used in further research

5.11.2 Pyruvate Kinase

A standard assay solution contained: 940 µl 50mM Tris/HCl buffer pH 6.5 at 70°C, 10 µl DTT 500 mM, 10 µl $MgCl_2$ 500 mM, 10 µl ADP 200 mM, 10 µl PEP 200 mM, 5 µl LDH, 10 µl NADH and 10 µl PK extract. A Hitachi U2010 spectrophotometer was used with a continues absorption measurement at 334 nm.
First the DTT, $MgCl_2$ and the ADP were added to the quarts cuvette, the machine was zeroed and the measurement was started. NADH, LDH and PEP were added and the background activity (PEP degradation) was determined. Finally the PK was added and the activity measured. At the end 10 µl of 500 mM pyruvate was added to make sure the auxiliary enzymes are not rate limiting.

5.11.3 Km determination

The activity of the PK was determined at different ADP concentration ranges (0.5, 1, 2 and 4 mM final concentration). This data was used to make a Lineweaver Burk plot. Using these results the Km value for ADP was calculated using the formula derived from the Lineweaver Burk plot.

6 Cloning Results

6.1 Restriction of pET24d and pMA plasmids

The result from the pET24d restriction is shown in figure 6.1. A restriction product of 5231bp and 76bp is expected. Only one fragment can be seen (5231bp). This is most likely because the 76 bp fragment has migrated off the gel.

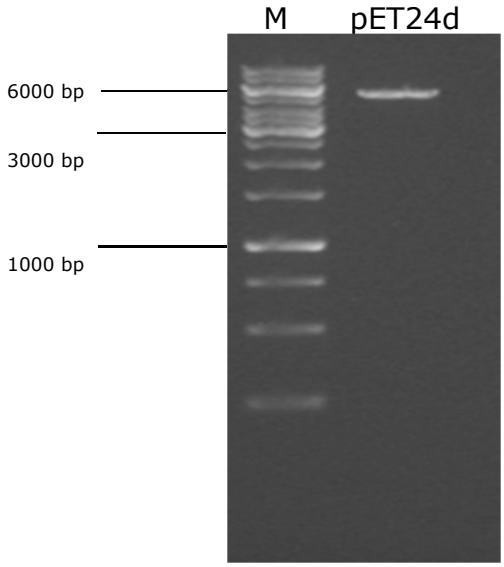

Figure 6-1 Marker (left) and pET24d restriction with XhoI and NcoI. Expected bands are at 5,2 kb and 76 bp. The large band can be seen whereas the short band is probably lost due to fast migration.

Table 6.1 shows the expected fragment size of the pMA vector restriction and figure 6.2 shows the restriction pattern from these vectors. The restriction pattern fits with the expectation, indicating a successful restriction. The proper fragment (gene) was isolated from the gel.

Table 6-1 Expected fragment sizes upon restriction of plasmids.

plasmid	pMA_1830	pMA_1831	pMA_1955	pMA_2366
Expected fragment size	971 2387	458 904 1008 1751	458 904 1008 2651	1250 2383

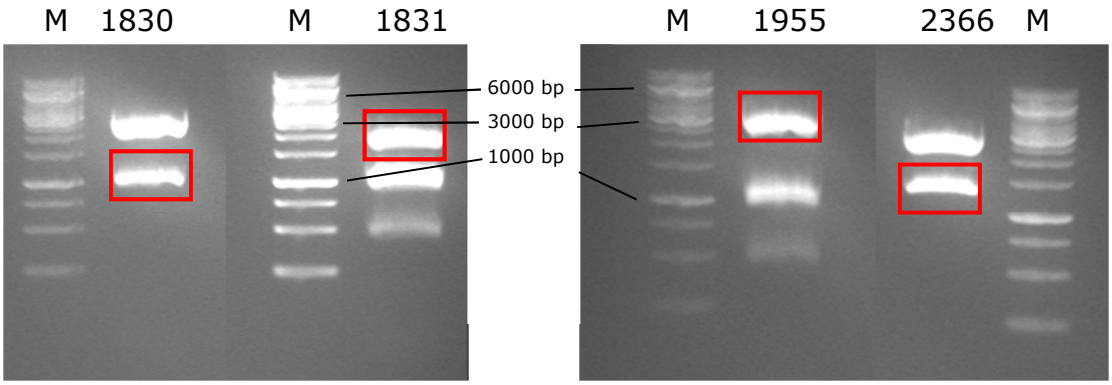

Figure 6-2 Fragmentation pattern of pMA plasmids. These fragments fit to the expectation. The marked bands are the genes of interest and are cut out from the gel. M stands for the marker which is a 1kb DNA ladder from Fermentas

6.2 Analysis of transformation products

The targeted bands (genes) were cut from the gel (figure 6.2) and purified. After ligation the constructs (pET24d_1830 etc.) were transformed to DH5α. Few colonies (>10) were found after the transformation. Control transformation with the background measurement showed less colonies (>3).

6.2.1 Colony PCR

The performed colony PCR did not show positive results (figure not shown). This was not further investigated.

6.2.2 Restriction analyses of constructs form transformation

A restriction analyses was performed on the same colonies from 6.2.1. The expected fragment sizes for each construct are shown in table 6.2. Restriction products are put on gel, figure 6.3. The restriction pattern is similar to the expected fragment size. This indicates the ligation was successful.

Table 6-2 Expected gene fraction after control restriction

plasmid	pET24d_ 1830	pET24d_ 1831	pET24d_ 1955	pET24d_ 2366
Expected bands (bp)	2248 3954	3028 3954	491 3437 3954	1250 5231

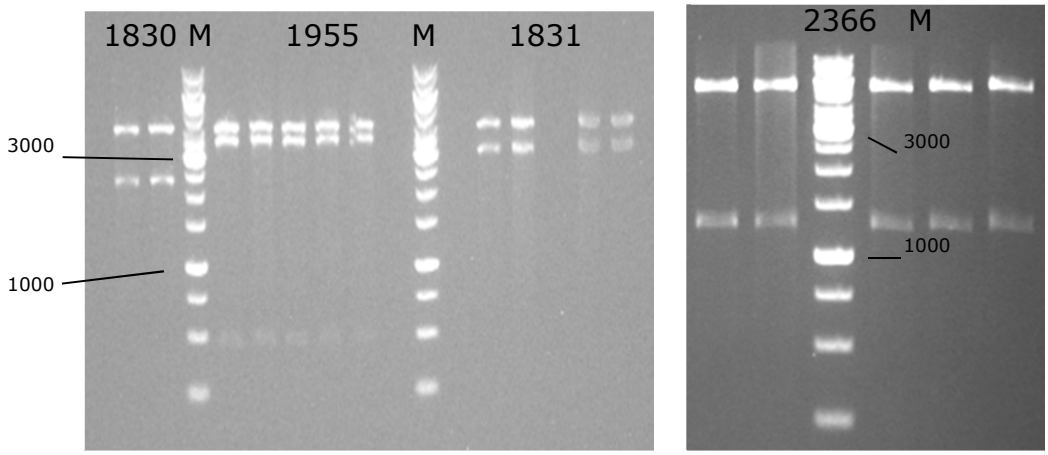

Figure 6-3 Restriction pattern of constructs. Left, Csac_1830, Csac_1831 and Csac_1955 were digested with XhoI and EcoRV. Right, Csac_2366 was digested with NcoI and XhoI. These patterns fit with the expectation. A 1 kb DNA ladder from fermentas was used as marker.

6.2.3 Sequence analysis of constructs

Isolated constructs from positive colonies from 6.2.2 were sent to BaseClear for sequencing. The sequencing data can be found in the digital attachment. The sequence data showed that no errors were made and that the gene is inserted in the correct direction. The his-tag and

start/stop codons are present at the right position and in the same reading frame as the inserted gene.

7 Protein expression and purification

The constructs (pET24d_1830, etc.) analysed during the previous chapter (6.2.1 - 6.2.3) were transformed to the production strain *E.coli* BL21de3. These transformants were cultivated and protein production was induced. The cells were lysed using a French press and the cell free extract (CFE) was obtained. This was heat treated and spun down and the heat stable cell free extract (HSCFE) was obtained.

7.1 Nickel column separation

The chromatograms following from FPLC runs with Nickel column are shown in figures 7.1, 7.3, 7.5 and 7.7. The expected pattern has an increase in UV absorption, conductivity measurement in the flow through and one peak during the salt gradient. The flow through contains proteins and DNA. During the salt gradient, the UV absorption will automatically increase due to high concentrations of imidazole.

ATP-PFK separation with the nickel column is shown in figure 7.1. The flow through runs from fraction 2-8, the elution peak falls between fractions 17-19, this pattern is as expected. Several fractions are put on SDS page gel figure 7.2. No proteins are visible in the flow through. This is due to the heat treatment, most of the cellular proteins are lost there. The absorption in the flow though is now mainly caused by DNA.
The SDS page gel clearly shows a band at the approximate size for ATP PFK (35 kDa). However two other bands (proteins) are also visible in fraction 18 at 15 and 25 kDa. No fractions were pooled.

The PPi PFK separation using the nickel column is shown in figure 7.3. The flow through falls in fraction 2-8. During the elution of the proteins from the column, two peaks can be distinguished: the first peak falls in fractions 18 and 19, the second falls in fractions 20-25.
Some fractions were put on SDS page gel, figure 7.4. A band corresponding to the height of the expected PPi PFK (47 kDa) is found in fractions 23 and 25. These fractions originate from the second peak. In the first peak, fractions 18, only a small protein was found at 15 kDa.
Fractions 20-25 were pooled. No other bands were seen in these fractions (figure 7.4, fraction 19, 23 and 25).

PK separation is shown in figure 7.5. The flow through (fraction 2-5) and during elution (fraction 16-22) both show two distinguishable peaks. Fractions are put on SDS gel, figure 7.6. A band with a similar height of PK (65 kDa) is found in fractions 16-23. Also, an additional band is seen in fraction 5 (flow through). This explains the second peak in the flow through. Other proteins can be found at approximately 25 kDa in the first peak of the elution (fractions 16 and 17).
Fractions 16-23 were pooled.

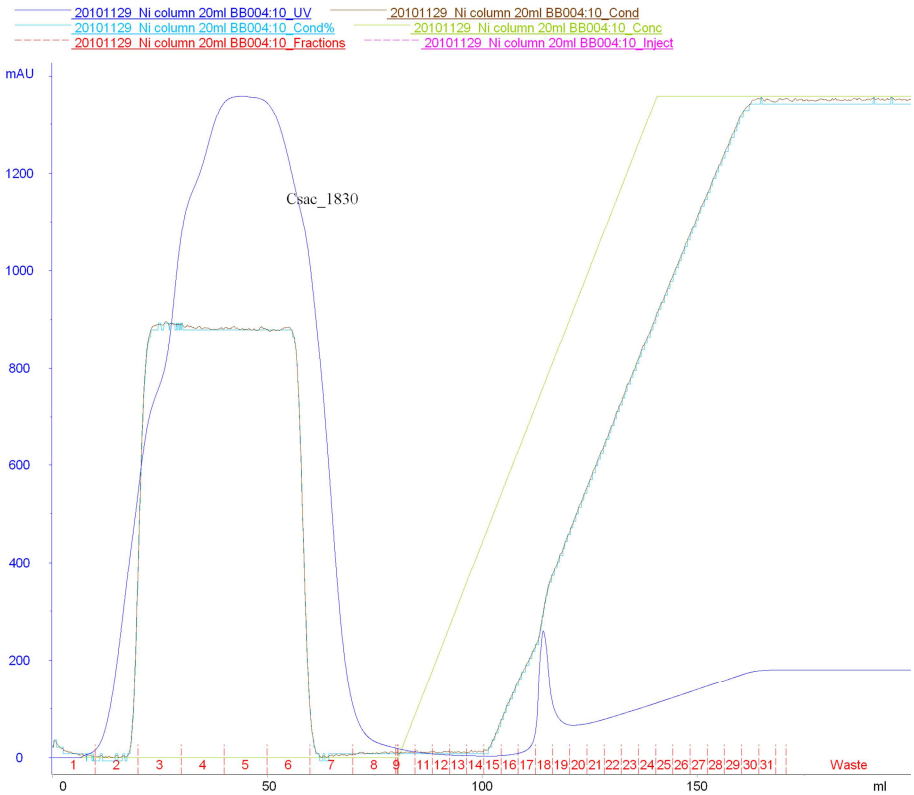

Figure 7-1 Chromatogram from Nickel column run. This sample contained the ATP-PFK. The red numbers on the bottom indicate the fraction, the purple line represents the absorption and the yellow/green line the mixing between buffer A and B. Finally, the brown line gives a measure of the conductivity

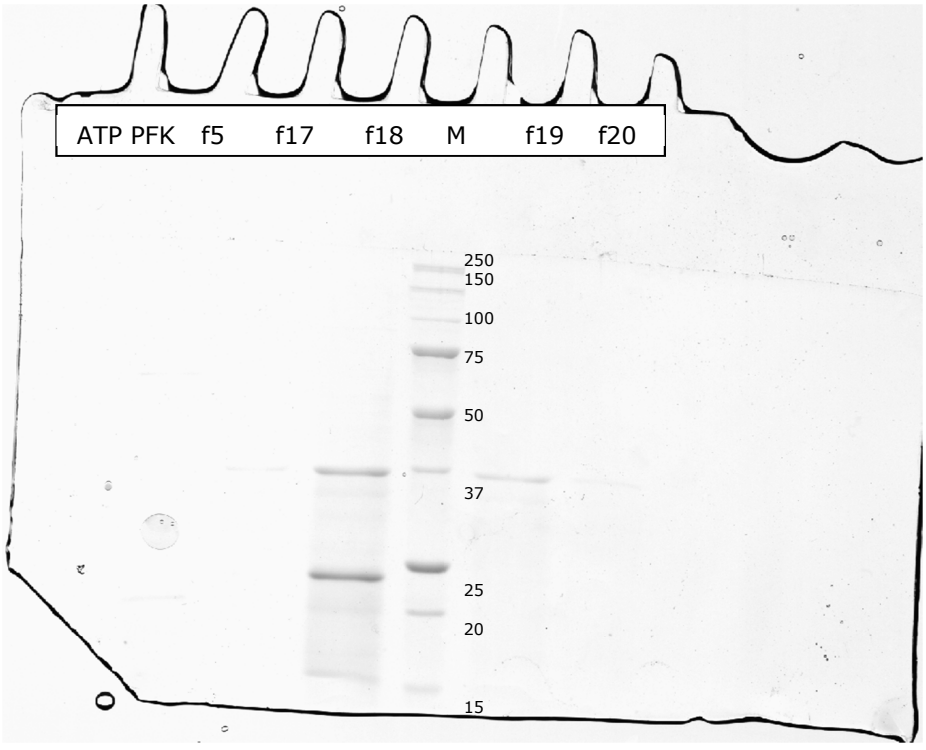

Figure 7-2 SDS gel of fractions of ATP PFK nickel column separation. Fraction numbers are indicated by fx, M is the marker. Fraction 5 is from the flow through, fractions 17 18 and 19 are from the elution peak. The expected protein size of ATP PFK is 35 kDa

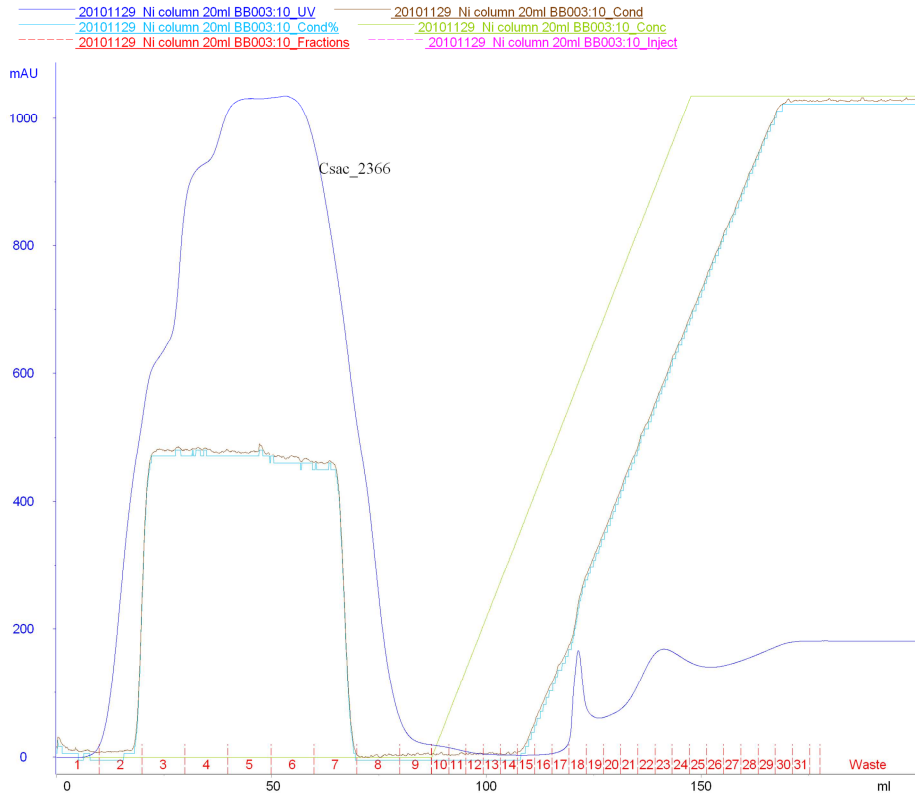

Figure7-3 Chromatogram from Nickel column run. This sample contained the PPi-PFK. The red numbers on the bottom indicate the fraction, the purple line represents the absorption and the yellow/green line the mixing between buffer A and B. Finally, the brown line gives a measure of the conductivity

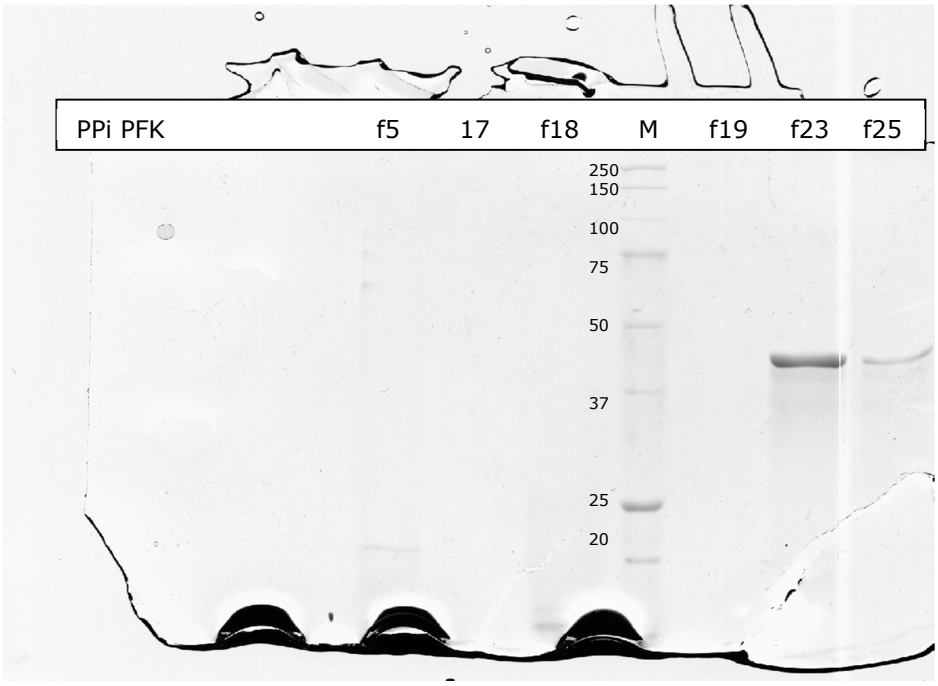

Figure 7-4 SDS gel of fractions of PPi PFK nickel column separation. Fraction numbers are indicated by fx, M is the marker. Fraction 5 is from the flow through, fraction 17 and 18 are from the first elution peak, fraction 19 is between the peak and fractions 23 and 25 are from the second elution peak. The expected high for a PPi PFK protein is 47 kDa.

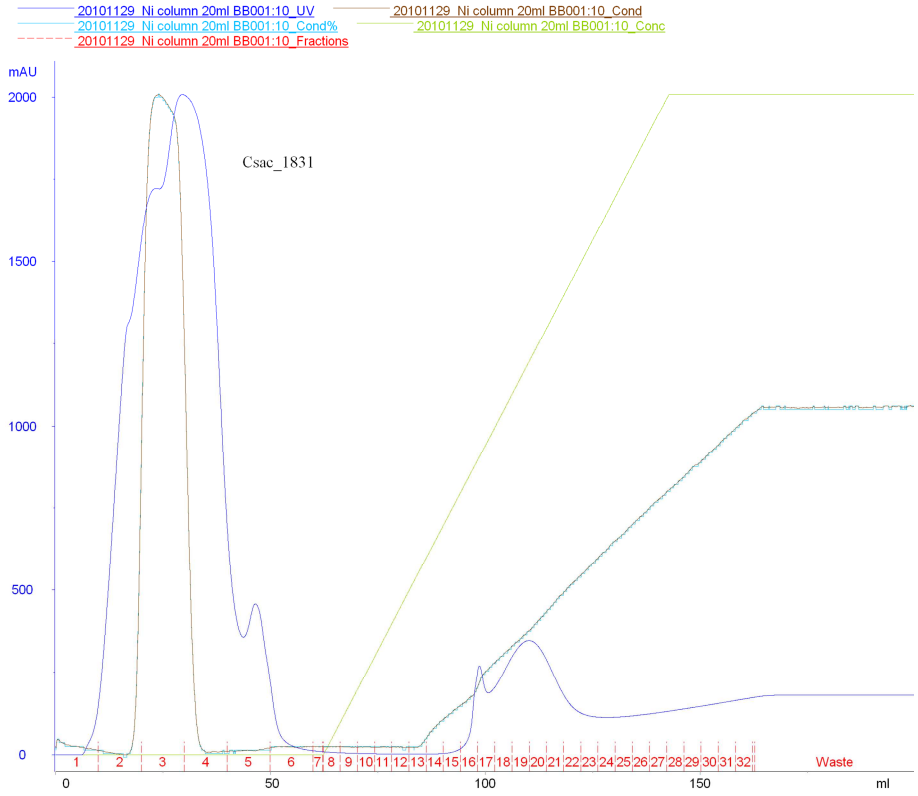

Figure 7-5 Chromatogram from Nickel column run. This sample contained the PK. The red numbers on the bottom indicate the fraction, the purple line represents the absorption and the yellow/green line the mixing between buffer A and B. Finally, the brown line gives a measure of the conductivity

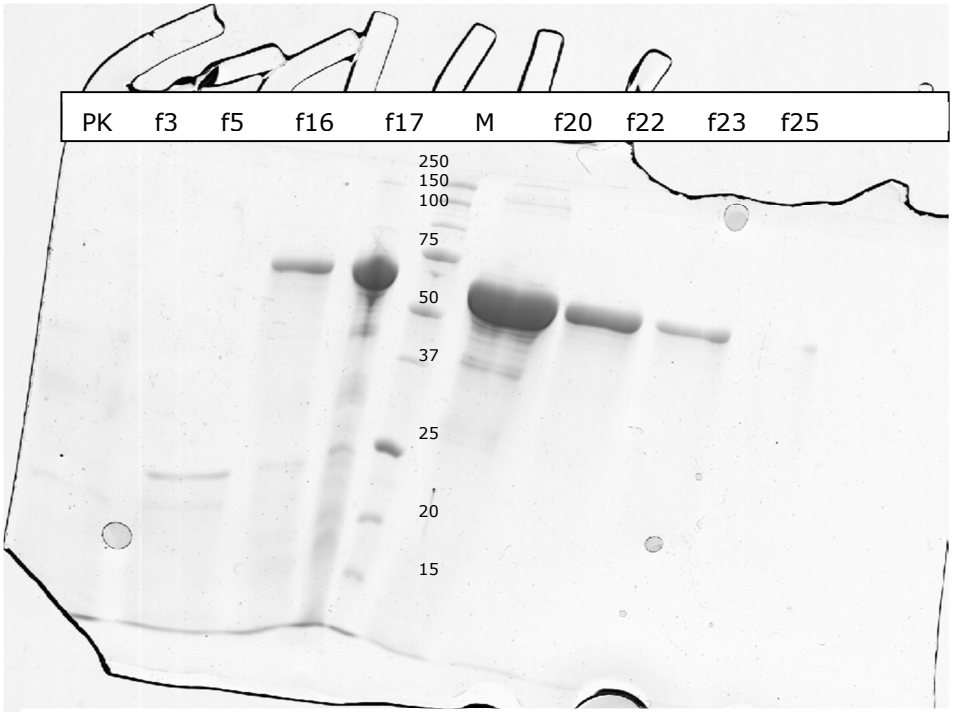

Figure 7-6 SDS gel of fractions of PK nickel column separation. Fraction numbers are indicated by fx, M is the marker. Fraction 3 and 5 are from the flow through, fraction 16 is from the first elution peak, fraction 17 can be an overlap between the first and second peak and fractions 20, 22 and 23 are from the second elution peak. Fraction 25 is after the second peak. The expected height for a PK protein is 65 kDa.

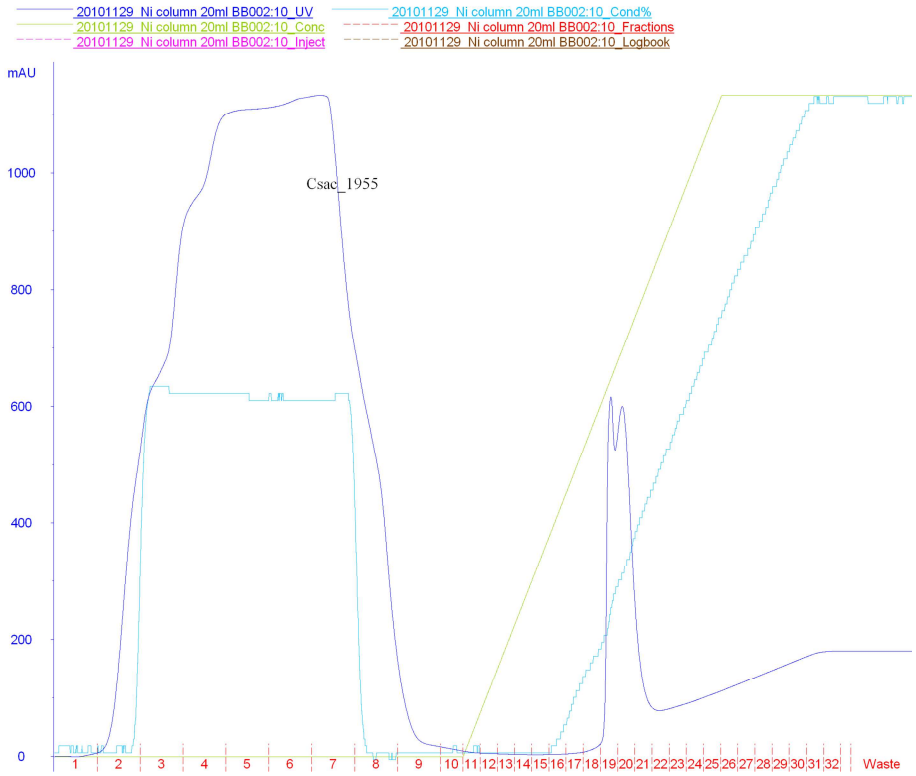

Figure 7-7 Chromatogram from Nickel column run. This sample contained the PPDK. The red numbers on the bottom indicate the fraction, the purple line represents the absorption and the yellow/green line the mixing between buffer A and B. Finally, the light blue line gives a measure of the conductivity

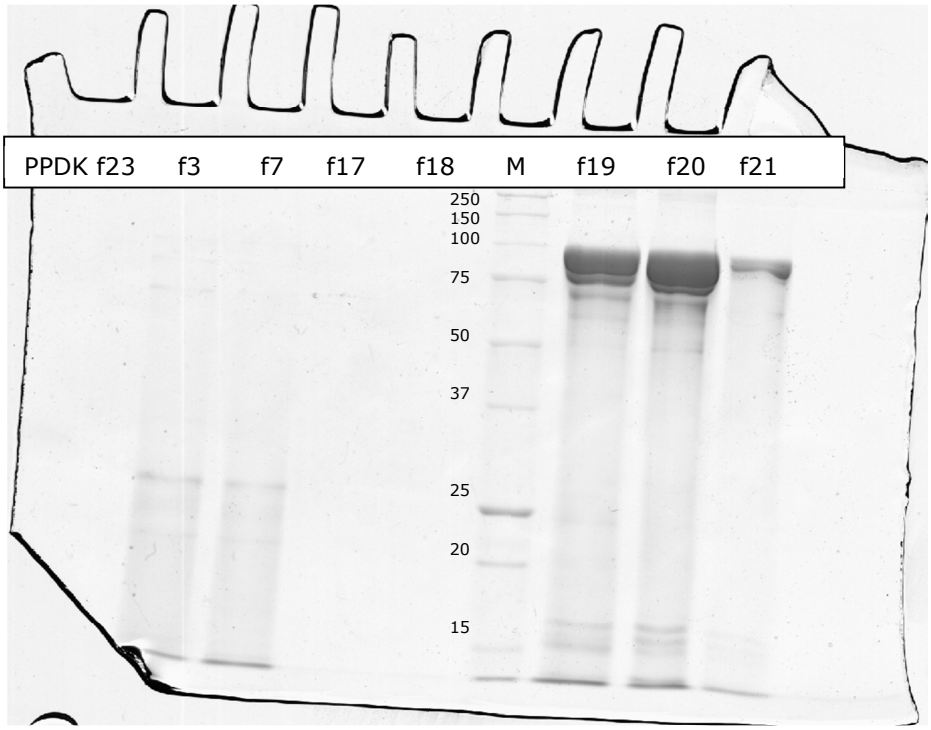

Figure 7-8 SDS gel of fractions of PPDK nickel column separation. Fraction numbers are indicated by fx, M is the marker. Fraction 3 and 7 are from the flow through, fraction 17 is before the peak, fraction 18 is the beginning of the first peak and fraction 19, 20 and 21 are the first and second peak (they overlap). The expected height for a PPDK protein is 100 kDa.

PPDK separation using a nickel column is shown in figure 7.7. The flow through is present in fraction 2-9. During elution two overlapping peaks (fraction 19-21) are visible. Several fractions were put on SDS page gel figure 7.8. Some protein is present in the flow through. In fractions 19-21 a clear band is visible matching the expected size of PPDK (100 kDa). In addition, some other bands are visible in these fractions in the range of 15-17 kDa. Fractions 19-21 were pooled.

7.2 Desalting

Fractions or pooled fractions from the nickel column purification were desalted. Table 11.1 (appendix 11.7) gives an overview of which desalting fractions contain which nickel column fractions. Additional information (desalting chromatogram) can be found in appendix 11.7, figures 11.9 and 11.10.

7.3 SDS analysis

SDS page gels were made showing different samples during purification (figures 7.9 to 7.12). Ideally the purified protein fraction should only show one band.

Clearly a lot of the putative ATP-PFK (35 kDa)is lost in the pellet of cell debris (figure 7.9). When the heat treatment is applied, even more of the putative ATP PFK is lost. The heat treatment is quite effective at removing cellular proteins from the sample. After the nickel column the putative ATP PFK band is hardly visible. However the proteins are no longer visible on the gel after desalting. This might be due to the fact that concentration differences were not taken into consideration during loading of the gel.

Figure 7.10 shows the purification results of the putative PPi PFK (47). In the nickel column fraction a band is still barely visible. However in the desalted fraction the concentration is too low to give a visible band. Strangely a different pattern can be seen in the heat treated pellet lane compared to the other lanes. Incidentally this is also the case in figure 7.11, which could indicate a pipetting error (swapping of samples).

PK purification is shown in figure 7.11. A lot of protein is still present after nickel column separation and desalting, even though a lot of putative PK protein (65 kDa) also ends up in the pellet. Some contamination with other proteins is still visible but the targeted PK protein is present in much higher quantities.

PPDK purification steps were put on SDS page gel. After the nickel column and the desalting steps the putative PPDK (100 kDa) is still abundant and quite pure. It seems that less protein is present in the HSCFE and the heat treated pellet compared to the nickel column fraction. This is likely to be a concentration difference due to a pipetting error.

All samples show a great increase in purity. Even though some additional bands are still present, these are present at much lower concentrations.

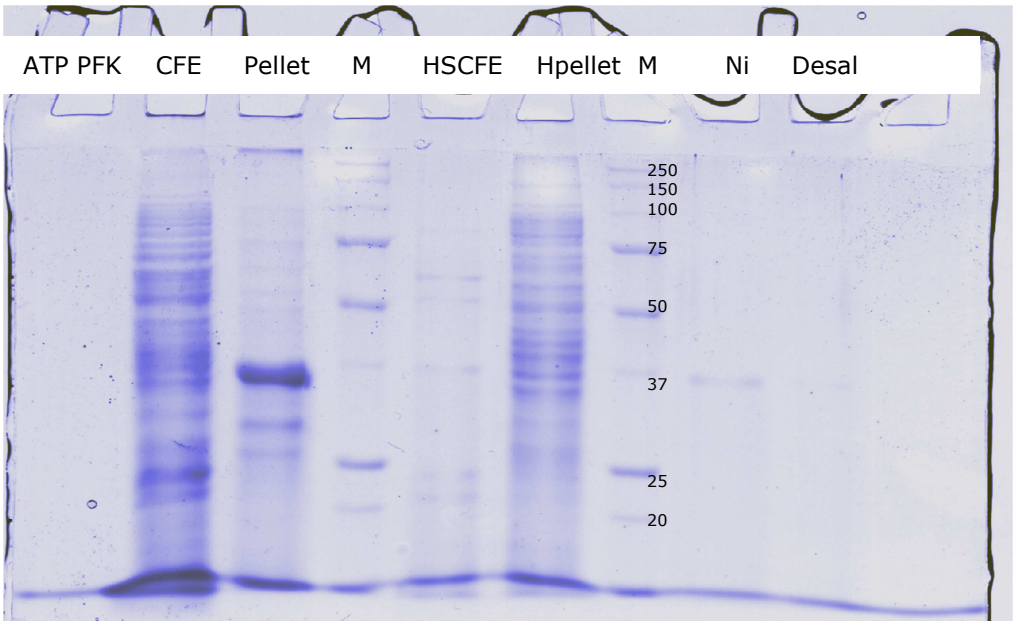

Figure 7-9 Samples after different isolation steps for the ATP-PFK. The expected protein size for this protein is 35 kDa. The abbreviations for the different lanes are: CFE stands for cell free extract(supernatant after cell rupturing), Pellet is the cell debris after cell rupturing. M stands for marker, HSCFE is the heat stable cell free extract, Hpellet is the pellet after heat treatment, Ni stands for nickel column and desal means the desalting portion.

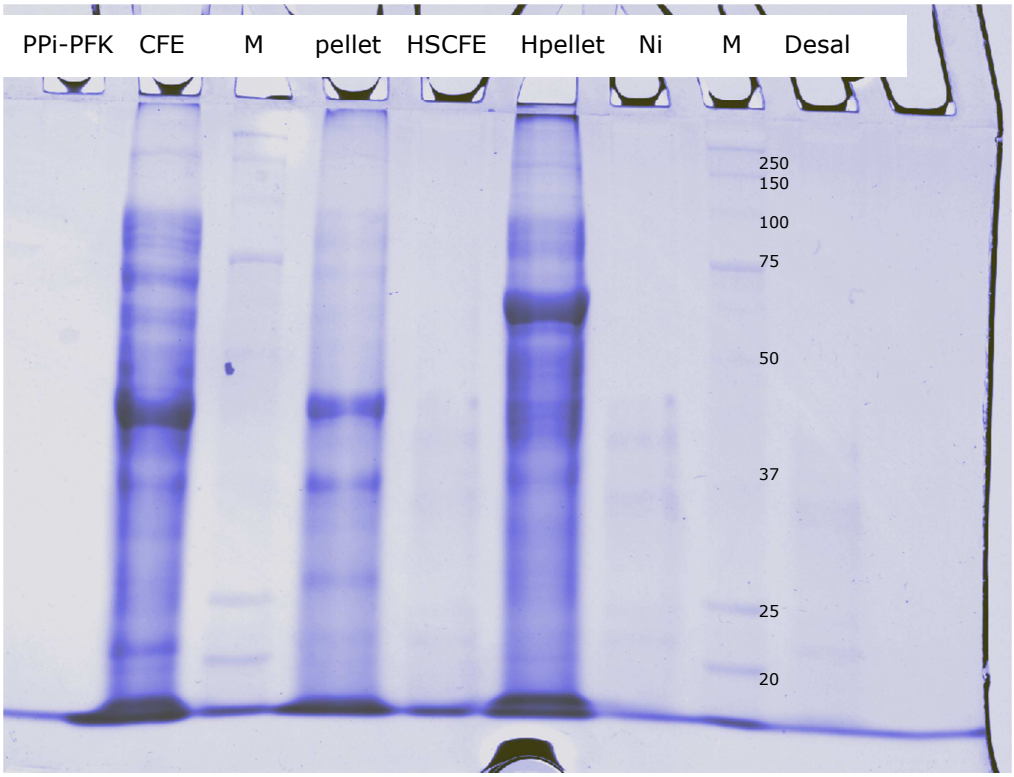

Figure 7-10 PPi-PFK samples at different points of isolation. The expected protein size for this protein is 47 kDa. The abbreviations for the different lanes are: CFE stands for cell free extract(supernatant after cell rupturing), Pellet is the cell debris after cell rupturing. M stands for marker, HSCFE is the heat stable cell free extract, extract, Hpellet is the pellet after heat treatment, Ni stands for nickel column and desal means the desalting portion.

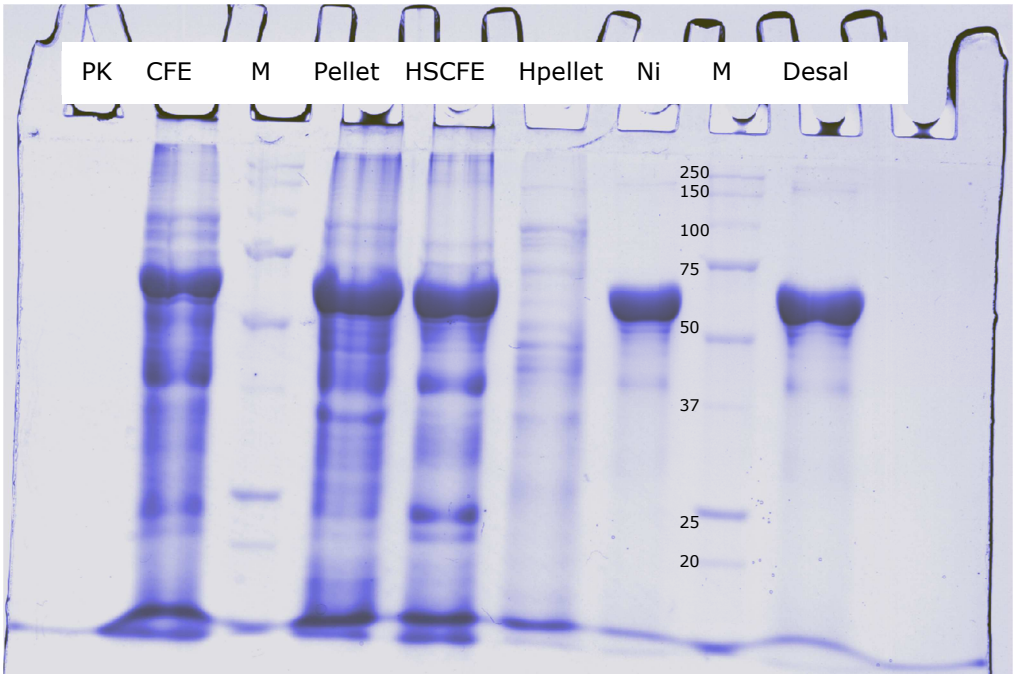

Figure 7-11 Samples after different isolation steps for the PK. The expected protein size for this protein is 65 kDa. The abbreviations of different lanes are:, CFE stands for cell free extract(supernatant after cell rupturing), Pellet is the cell debris after cell rupturing. M stands for marker, HSCFE is the heat stable cell free extract, Hpellet is the pellet after heat treatment, Ni stands for nickel column and desal means the desalting portion.

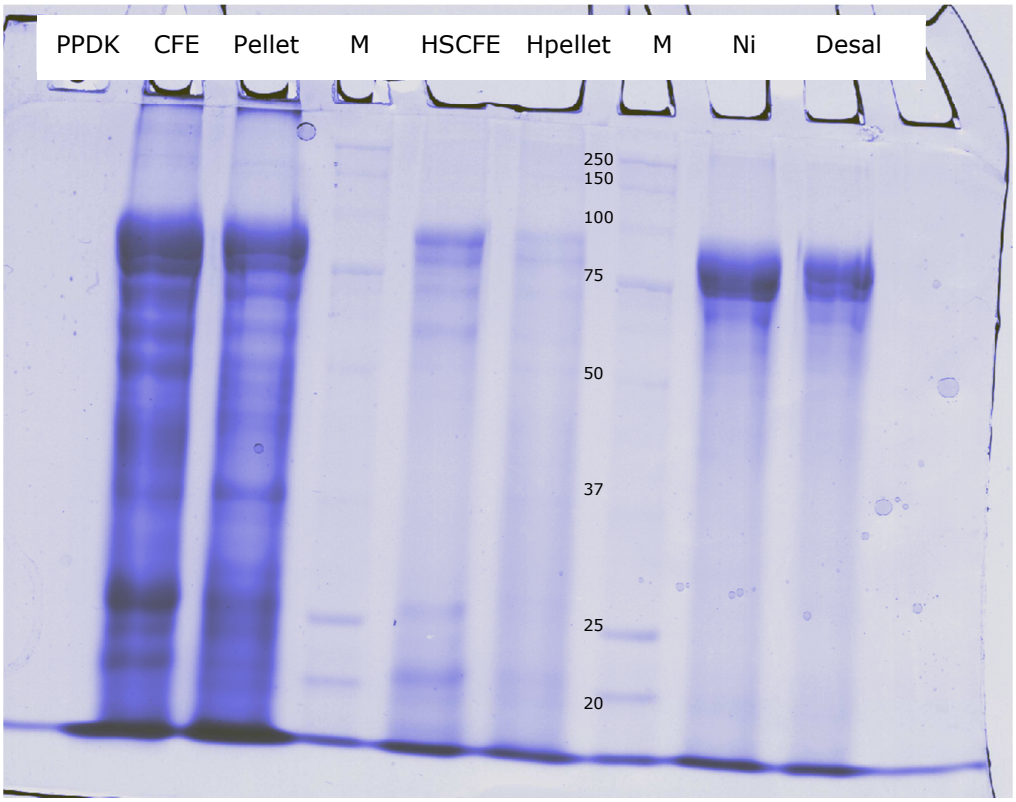

Figure 7-12 PPDK samples at different points of isolation. The expected protein size for this protein is 100 kDa. The abbreviations of the different lanes are: CFE stands for cell free extract(supernatant after cell rupturing), Pellet is the cell debris after cell rupturing. M stands for marker, HSCFE if the heat stable cell free extract, Hpellet is the pellet after heat treatment, Ni stands for nickel column and desal means the desalting portion.

7.4 Superdex analysis of purified proteins

The purified proteins were tested for multimers using a superdex column A calibration was performed on the superdex (shown in appendix 11.8 figure 11.11, 11.12 and 11.13). The calibration curve shown in figure 7.11 is derived.

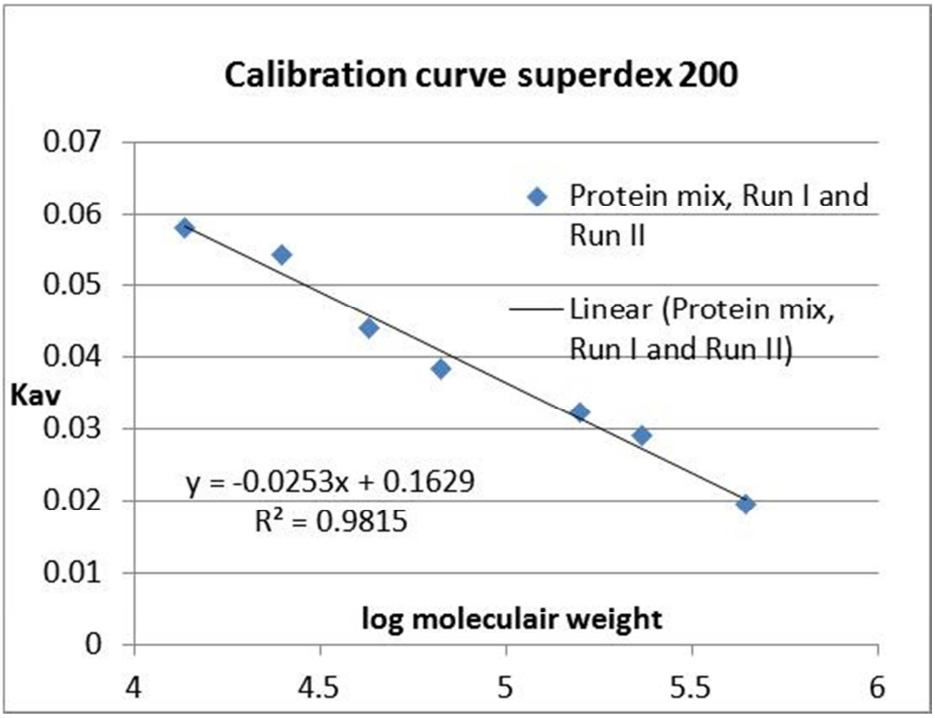

Figure 7-11 Calibration curve from superdex column. The x-axis represents the log of the molecular weight of the proteins, while the y-axis shows the value Kav ((Ve-Vo)/(Vt-V0)) whereas Ve= elution volume of the proteins, v0= void volume (determined by Blue dextran elution = 7ml) and Vt= the total bed volume (200ml)

Appendix 11.9, figure 11.14 to 11.17, show the superdex chromatograms for the isolated proteins. Using the formula obtained from the calibration curve the molecular weights corresponding to the different peaks are calculated and are shown in table 7.2

Table 7-1 protein size calculated from superdex analysis

Protein	***ATP PFK***	***PPi PFK***	***PK***	***PPDK***
kDa	84 19	286 39	286	286
Expected kDa	35	47	65	100

None of the targeted proteins are found on the superdex analysis. The 286 kDa protein is likely to be some kind of contaminant. Since this size does not correspond to any poly-form of these proteins, and it is present in three of the four samples it could have been accidentally introduced at

some point. The smaller protein present in the ATP PFK and PPi PFK is likely to be an *E.coli* cellular protein.

7.5 Total Protein

A calibration of the Roti-Nanoquant is made and shown in table 11.2 (appendix 11.10).
Plotting these results the following formula is derived y = 0.017x + 0.47 with R^2 of 0.99.
Using this formula the concentration of protein in the samples was calculated and is shown in table 7.2.

Table 7-2 Results from Roti-Nanoquant total protein determination. The average concentration gives the corrected and averaged values from the diluted samples. Also the standard deviation and the variation quotient are given.

Enzyme name	Average µg/ml	St dev
PK	291.6	43.1
PPDK	430.9	7.2
ATP PFK	116.5	22.4
PPi PFK	93.7	16.4

8 Enzymatic characterization

Purified and desalted proteins (7.2) were used in for characterization studies.

8.1 Preliminary activity assay

Activity assays on the unpurified cell free extract showed an activity for the ATP PFK enzyme. This activity ranged from 0.02 to 0.07 absorption/min (results not shown).

8.2 pH optimum exploration

Table 8-1, the activity of PK at different pH values is given. pH 6.48 results in the highest activity (µmol/min*mg). This pH is used in further assays.

Table 8-1 Activity of PK at different pH values

pH	*Activity (µmol/min*mg)*
6.05	1485
6.48	2018
7.03	193
7.43	808

8.3 Km value determination ADP on PK

Activity measurements of PK were performed with varying ADP concentrations. A Lineweaver Burk plot was made, figure 8.1.
Using the Lineweaver Burk plot, the Vmax and Km values were calculated, table 8.2.

Table 8-2 calculated Vmax (*µmol/min*mg*) en Km (mM) according to the Lineweaver Burk Plot.

Vmax (µmol/min*mg)	*Km (mM)*
11111	2.22

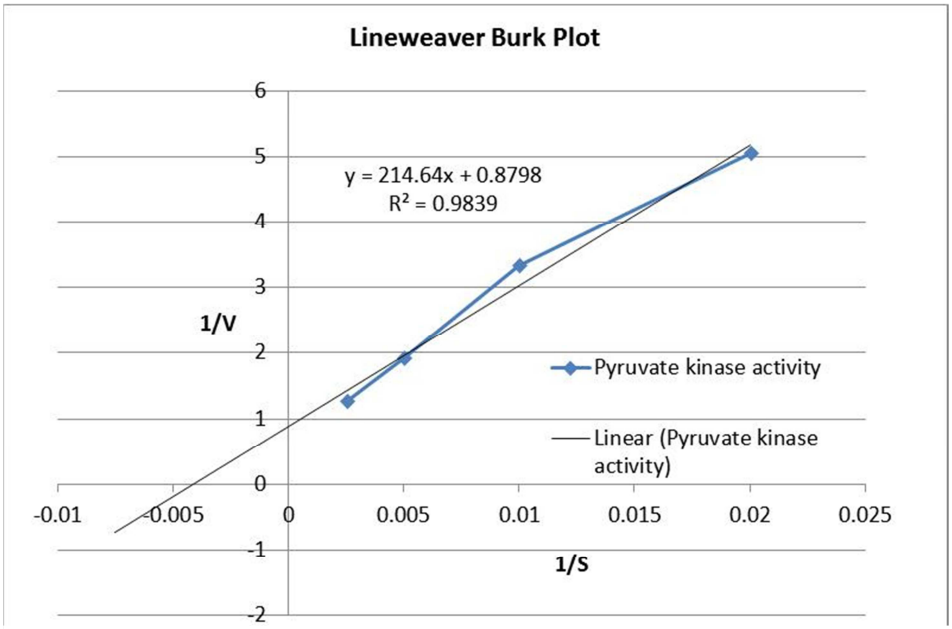

Figure 8-1 Lineweaver Burk plot. Using the formula, the Km and Vmax can be calculated. The interception point of the x-axis = -1/Km, while the interception point of the y-axis – 1/Vmax.

9 Discussion, Conclusions and Recommendation

9.1 Genetic work

In conclusion of the cloning experiments, a successful cloning of the different *C.saccharolyticus* genes into separate pET24d plasmids was achieved (see restriction analysis section 6.2.2, figure 6.3 and the sequence analysis, section 6.2.3).

Although it is not mentioned in this report, it has been found that the method of cloning and transformation is pivotal for the success rate of the afore mentioned experiments. Clear as this may be, subtle changes that were not assumed to play a large role in the outcome of the experiments, did prove to play a role. For instance, it was found that only when the genes were isolated from gel, the pET24d plasmid was treated with Antarctic Phosphatase after restriction and a heat shock with commercially competent cell was performed, positively transformed colonies were present.
Experiments where the genes were isolated from gel, but the pET24d plasmid not treated with Antarctic Phosphatase and an electroshock used as transformation technique did not results in transformed colonies. Neither did the use of Antarctic Phosphatase on the insert without isolation from gel in combination with untreated, digested vector and electroshock transformation. While this combination may indeed be the most efficient method, only the fragment of interest is isolated from gel and self ligation of the plasmid is prevented by Antarctic Phosphatase, it would be expected that without these methods the transformation efficiency would lower whereas in this case it seems a prerequisite for transformation.

When making a genetic construct, or performing any other experiment which does not involve the actual research question most researchers often use a ´quick and dirty´ method. This was also the case for this research. When this method is successful it is a very fast way to reach the point where the real research questions can be addressed. However this speedy approach does not include a lot of control steps, with the exception of a final control. Hence, when the ´quick and dirty´ method fails it is quite hard to pinpoint the error. And since the will to address the actual research questions can be quite large, it requires several failing experiments before the focus is switched to this start-up experiment. Therefore it can take quite some time before a well balanced experiment with proper controls is set up and executed. This is the ever present risk of a 'quick and dirty' experiment changing into a 'slow and dreadful'.

9.2 Protein production and isolation

Based on the protein production and isolation experiments it can be concluded that all the proteins were produced (figure 7.2, 7.4, 7.6 and 7.8). This means the method of induction is effective. Also the proteins are reasonably pure, there is some contamination left but this is

substantially less than the protein of interest (estimated from figure 7.2, 7.4, 7.6 and 7.8). The heat treatment is a very efficient method to reduce the amount of cellular proteins from the cell free extract since the flow through of the nickel column (see afore mentioned figures) is as good as protein free.

Even though proteins are produced, the overall recovery is not very high (table 7.2). As becomes clear from figure 7.9 to 7.12, a lot of protein is lost during centrifugation of the cell free extract and the heat treatment. Still optimization of the production and isolation seems a bit redundant since at least the pyruvate kinase had to be diluted ten times during the initial enzyme assays.

As mentioned above, quite a lot of protein remains in the cell free extract. By estimation from gel (7.9 to 7.12) this is up to 50% of the total protein produced. It is possible that inclusion bodies or aggregates are formed, this might be caused for instance by a lack of certain chaperones (Fink 1998).
Naturally attempts can be made to increase the overall yield by trying to recover these inclusion bodies (Singh and Panda 2005), but these methods are likely quite time consuming and one should wonder if this is really necessary in this research setting. Purely speculative it might be helpful to perform a heat treatment prior to the French press as this might cause the proteins to fold properly and remain in the supernatant after the cells are disrupted. Another possibility is to clone additional chaperone proteins into the production strain, or to give the cell a small heat or cold shock to trigger the formation of native HSP proteins. Or simply, the concentration of IPTG can be lowered to achieve a lower induction.

When analysis the proteins on the superdex column, the proteins of interest cannot be found. This is strange because proteins of other sizes can be detected, while the protein of interest is more abundant. Also no multimer of a particular protein is found. One possibility is that accidentally the same sample was loaded repeatedly. Another point that stands out is the deviation when the calibration proteins are recalculated with the calibration curve. These variation deviated between 37 kDa and 0.2 kDa from the original molar mass. Variation of this size make an accurate estimation rather difficult.

9.3 Enzyme assays

The PK and the ATP PFK showed activity during enzyme assays. Thus at least these enzymes were actively produced. The other two enzymes were not yet tested.

Enzyme assays with the Pyruvate kinase proved to be more of a challenge than initially anticipated. For starters, phosphoenolpyruvate (PEP) is slowly degraded at ambient temperatures, but this process is faster at higher temperatures. Since the enzyme assays take place at 70 ^{o}C the degration of PEP needs to be measured as a background, before starting the actual enzyme measurement. As a final control is also required, this

pose a challenge since an adequate measurement of the degration, the actual enzyme activity and the check on the auxiliary enzymes needs to be performed while there is only a limited amount of NADH. For these experiments it was found that a measurement of 100 seconds where the last 50 seconds were used for the degradation and 50 seconds where the last 30 seconds were used for the actual activity was enough to obtain reproducible results.
When determining Km values for ADP, problems with regard to Mg^{2+} precipitation where observed. Since ADP needs to form a complex with Mg^{2+} (Gupta and Benovic 1978) in order to be handled by the enzymes, they need to be present on a 1: 1 basis. However, concentrations of 6 mM and above resulted in precipitation in the reaction mix.
So far, initial concentration of PPi (0.4 mM) and Mg^{2+}(1mM) also result in precipitation

9.4 Future recommendation

In the future, when performing standardized experiments such as the cloning of several genes into a new plasmid, when a first 'quick and dirty' method fails it is impeditive to set up a proper experiment with the second try. Instead of trying to increase the amount controls at every try.

During activity assays quite some trouble is experienced due to precipitation. A logical test would be to lower the concentrations until no precipitation is visible. Since ADP (or PPi) form a complex with Mg^{2+} their concentrations need to be raised or lowered on a 1:1 basis.

If research on this topic would be continued the author of this report thinks it is advisable to redo the experiments from the pET24d_gene constructs. Since current enzyme stock are already several months old, it seems logical to make a fresh stock. Hopefully this thesis can be helpful when experiments are repeated.

10 References

Aust, A. E. and C. H. Suelter (1978). "Homogeneous pyruvate kinase isolated from yeast by two different methods is indistinguishable from pyruvate kinase in cell-free extract." Journal of Biological Chemistry **253**(20): 7508-7512.

Bárcena, M., M. Radermacher, et al. (2007). "The structure of the ATP-bound state of S. cerevisiae phosphofructokinase determined by cryo-electron microscopy." Journal of Structural Biology **159**(1): 135-143.

Bielen, A. A. M., K. Willquist, et al. (2010). "Pyrophosphate as a central energy carrier in the hydrogen-producing extremely thermophilic Caldicellulosiruptor saccharolyticus." Fems Microbiology Letters **307**(1): 48-54.

BRENDA. (2011). "Brenda Enzyme Database." Retrieved 14-3, 2011, from http://www.brenda-enzymes.org/.

Claassen, P. A. M., T. de Vrije (2006). "Non-thermal production of pure hydrogen from biomass: HYVOLUTION." International Journal of Hydrogen Energy **31**: 1416 – 1423.

de Vrije, T., A. E. Mars, et al. (2007). "Glycolytic pathway and hydrogen yield studies of the extreme thermophile Caldicellulosiruptor saccharolyticus." Applied Microbiology and Biotechnology **74**(6): 1358-1367.

Ding, Y.-H. R., R. S. Ronimus, et al. (2001). "Thermotoga maritima Phosphofructokinases: Expression and Characterization of Two Unique Enzymes." J. Bacteriol. **183**(2): 791-794.

Fink, A. L. (1998). "Protein aggregation: folding aggregates, inclusion bodies and amyloid." Folding and Design **3**(1): R9-R23.

Fridleifsson, I. B. (2003). "Status of geothermal energy amongst the world's energy sources." Geothermics **32**(4-6): 379-388.

Gupta, R. K. and J. L. Benovic (1978). "Magnetic resonance and kinetic studies of the spatial arrangement of phosphoenolpyruvate and chromium (III)-adenosine diphosphate at the catalytic site of pyruvate kinase." Journal of Biological Chemistry **253**(24): 8878-8896.

Johnsen, U., T. Hansen, et al. (2003). "Comparative Analysis of Pyruvate Kinases from the Hyperthermophilic Archaea Archaeoglobus fulgidus, Aeropyrum pernix, and Pyrobaculum aerophilum and the Hyperthermophilic Bacterium Thermotoga maritima." Journal of Biological Chemistry **278**(28): 25417-25427.

Kotlarz, D. and H. Buc (1981). "Regulatory Properties of Phosphofructokinase 2 from Escherichia coli." European Journal of Biochemistry **117**(3): 569-574.

Lindell, T. J. and E. Stellwagen (1968). "Purification and Properties of Phosphofructokinase from Yeast." Journal of Biological Chemistry **243**(5): 907-912.

Mertens, E. (1991). "Pyrophosphate-dependent phosphofructokinase, an anaerobic glycolytic enzyme?" FEBS Letters **285**(1): 1-5.

Novagen. (2011). "pET vector table." Retrieved 15-3, 2011, from http://www.merck-chemicals.nl/life-science-research/vector-table-novagen-pet-vector-table/c_HdSb.s1O77QAAAEhPqsLdcab?PortalCatalogID=merck4biosciences&CountryName=Netherlands.

O'Brien, W. E., S. Bowien, et al. (1975). "Isolation and characterization of a pyrophosphate-dependent phosphofructokinase from

Propionibacterium shermanii." Journal of Biological Chemistry **250**(22): 8690-8695.
OpenWetWare. (2011). "E.coli genotypes." Retrieved 15-3, 2011, from http://openwetware.org/wiki/E._coli_genotypes#BL21.28DE3.29.
Pendergrass, D. C., R. Williams, et al. (2006). "Mining for allosteric information: Natural mutations and positional sequence conservation in pyruvate kinase." IUBMB Life **58**(1): 31-38.
Peng, Z.-Y. and T. E. Mansour (1992). "Purification and properties of a pyrophosphate-dependent phosphofructokinase from Toxoplasma gondii." Molecular and Biochemical Parasitology **54**(2): 223-230.
Rainey, F. A., A. M. Donnison, et al. (1994). "Description of Caldicellulosiruptor saccharolyticus gen. nov., sp. nov: an obligately anaerobic, extremely thermophilic, cellulolytic bacterium." FEMS Microbiol Lett **120**(3): 263-266.
Rajvanshi, A. K. (1986). Alternative Energy in Agriculture.
Rostrup-Nielsen, J. R. (2005). "Making Fuels from Biomass." Science **308**(5727): 1421-1422.
Saavedra, E., R. Encalada, et al. (2005). "Glycolysis in Entamoeba histolytica." FEBS Journal **272**(7): 1767-1783.
Schlapbach, L. and A. Zuttel (2001). "Hydrogen-storage materials for mobile applications." Nature **414**(6861): 353-358.
Shafiee, S. and E. Topal (2009). "When will fossil fuel reserves be diminished?" Energy Policy **37**(1): 181-189.
Siebers, B., H.-P. Klenk, et al. (1998). "PPi-Dependent Phosphofructokinase from Thermoproteus tenax, an Archaeal Descendant of an Ancient Line in Phosphofructokinase Evolution." J. Bacteriol. **180**(8): 2137-2143.
Singh, S. M. and A. K. Panda (2005). "Solubilization and refolding of bacterial inclusion body proteins." Journal of Bioscience and Bioengineering **99**(4): 303-310.
Sissons, C. H., K. R. Sharrock, et al. (1987). "Isolation of Cellulolytic Anaerobic Extreme Thermophiles from New Zealand Thermal Sites." Appl Environ Microbiol **53**(4): 832-838.
Sugiyama, T. (1973). "Purification, molecular, and catalytic properties of pyruvate phosphate dikinase from the maize leaf." Biochemistry **12**(15): 2862-2868.
Uyeda, K. and S. Kurooka (1970). "Crystallization and Properties of Phosphofructokinase from Clostridium pasteurianum." Journal of Biological Chemistry **245**(13): 3315-3324.
van de Werken, H. J., M. R. Verhaart, et al. (2008). "Hydrogenomics of the extremely thermophilic bacterium Caldicellulosiruptor saccharolyticus." Appl Environ Microbiol.
van Niel, E. W. J., P. A. M. Claassen, et al. (2003). "Substrate and product inhibition of hydrogen production by the extreme thermophile, Caldicellulosiruptor saccharolyticus." Biotechnology and Bioengineering **81**(3): 255-262.

11 Appendix

11.1 Gene ruler and protein marker

Gene ruler

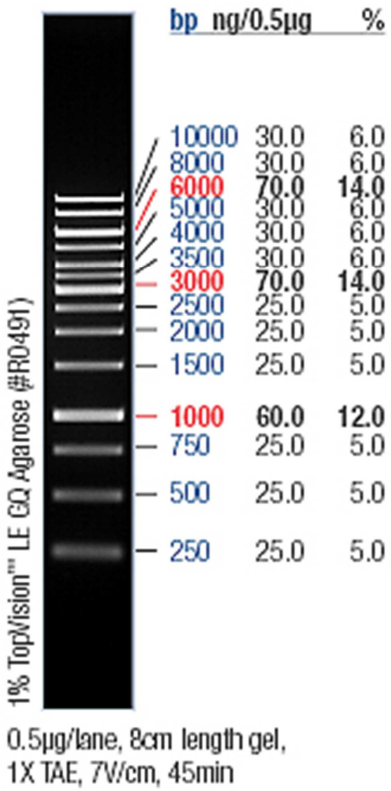

Protein marker

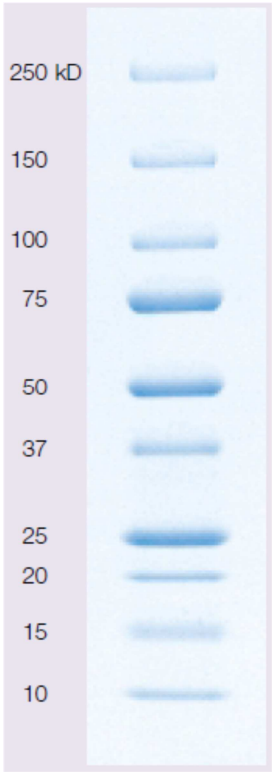

Figure 11-1 left, 1kb DNA ladder (fermentas) that was used to estimate the DNA band size on agarose gel. Right, protein marker (Bio-Rad) that was used as ruler for SDS page

11.2 pET24d destination vector

Figure 11-2 and Figure 11-3 illustrate the pET24d plasmid and at which positions the plasmid is cut.

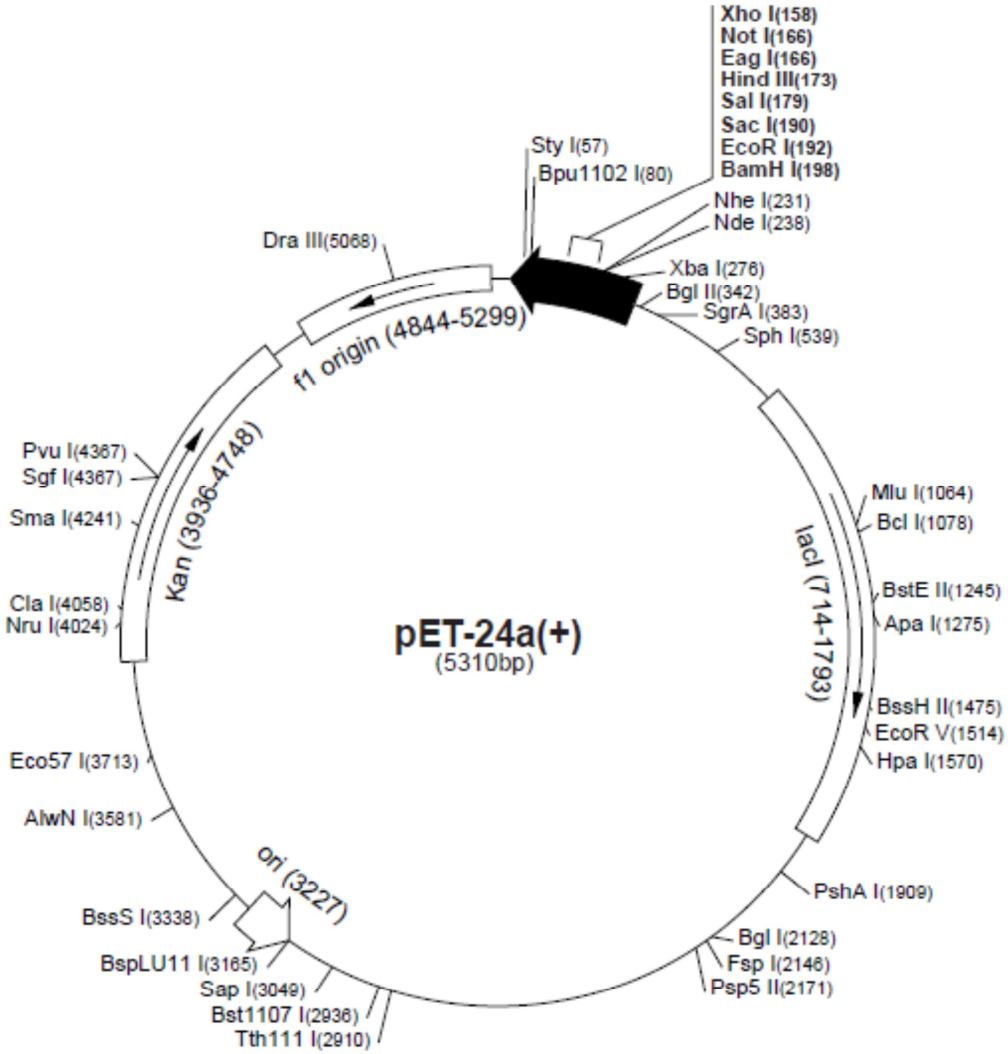


```
pET-24d
      NcoI
...TACCATGGCTAGC...
      MetAlaSer...

pET-24b   ...GGTCGGGATCCGAATTCGAGCTCCGTCGACAAGCTTGCGGCCGCACTCGAGCACCACCACCACCACCACTGA
          ...GlyArgAspProAsnSerSerSerValAspLysLeuAlaAlaAlaLeuGluHisHisHisHisHisHisEnd

pET-24c,d ...GGTCGGATCCGAATTCGAGCTCCGTCGACAAGCTTGCGGCCGCACTCGAGCACCACCACCACCACCACTGA
          ...GlyArgIleArgIleArgAlaProSerThrSerLeuArgProHisSerSerThrThrThrThrThrGlu
```

Figure 11-2 Plasmid map of pET24d plasmid (above). (below) The plasmid contains a NcoI restriction site as well as a XhoI site which will place the gene directly in front of a His-tag (CAC repeat) followed by a TGA end sequence.

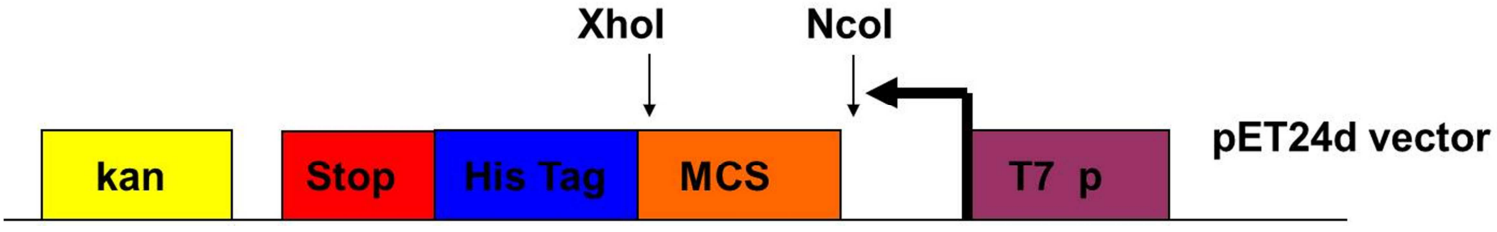

Figure 11-3 graphical illustration of pET24d restriction. The MCS that is cut out is 76 bp.

11.3 pMA plasmid

pMA plasmid map, Figure 11-4, and restriction organization, Figure 11-5. NcoI and BsphI result in the same overhang and can thus be fused together. However the recombined DNA cannot be digested by either of the restriction enzymes.

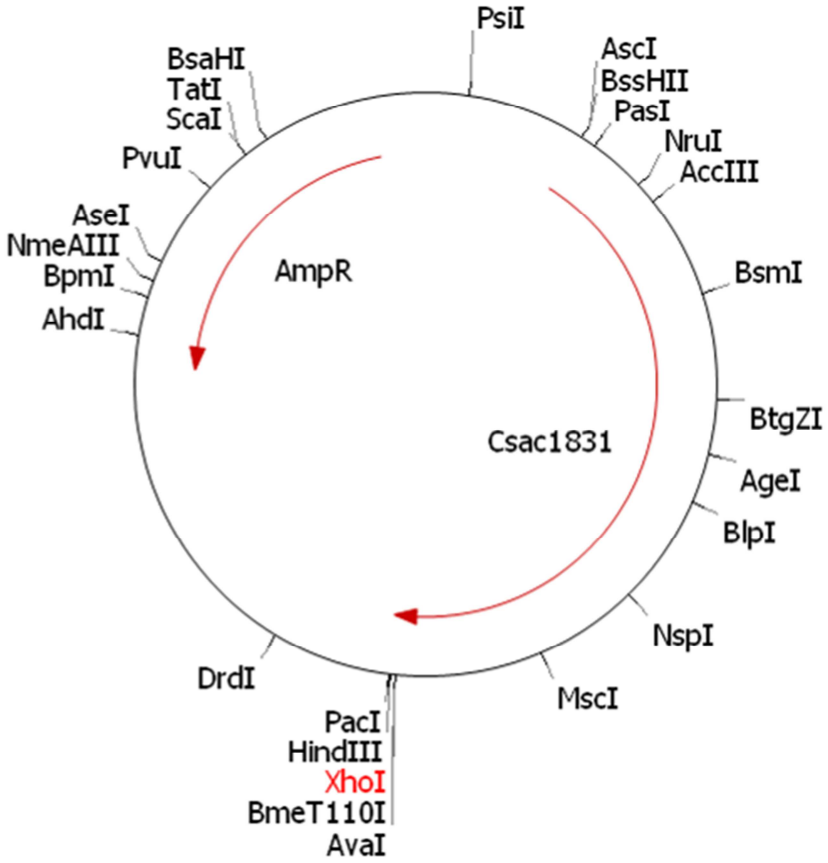

Figure 11-4 pMA plasmid containing one of the *Caldicellulosiruptor saccharolyticus* genes. At the 3' end a restriction site for either NcoI or BsphI was situated (generating the same overhang). At the 5' end an XhoI site is present

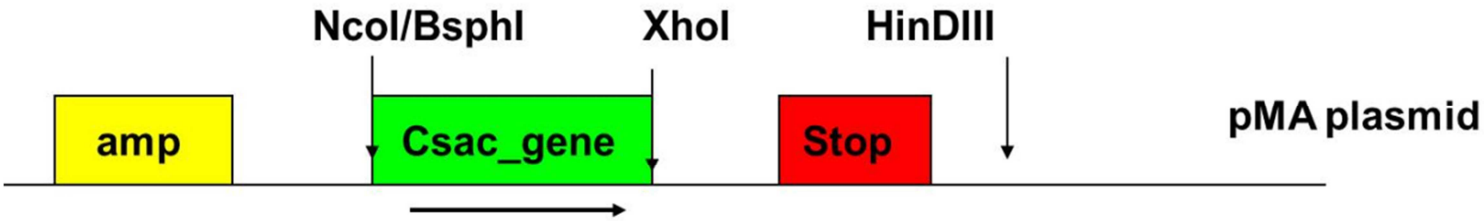

Figure 11-5 Organization of pMA plasmid. The restrictions of NcoI and BsphI result in the same overhang. Normally XhoI is used but optionally HinDIII can be used. This will result in a protein not fused to the HIS tag.

11.4 Visualization of ligation

Figure 11-6 illustrates the organization of the construct. The gene is in frame with the HIS tag and the stop codon. The T7 promotor can be activated by T7 RNA polymerase which in turn can be transcribed by IPTG (11.11.3)

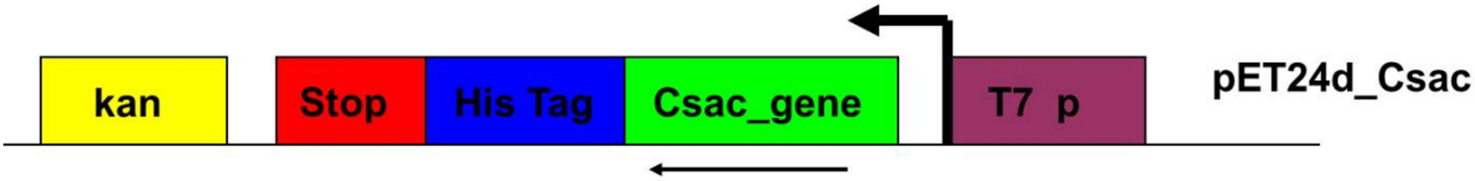

Figure 11-6 Above, this picture illustrates the construct after ligation. Below, a display of the restriction sites. Some constructs will have a recombined site NcoI/BsphI. Due to the recombination, neither of the enzymes will digest this site.

Recombined NcoI/BsphI site	pET24d NcoI	XX C| CATG A XX XX G GTAC|T XX Csac_gene BsphI
Non-recombined NcoI site	pET24d NcoI	XX C| CATG G XX XX G GTAG|G XX Csac_gene NcoI
XhoI site	pET24d XhoI His-tag	GTG C| TCGA G XX CAC G AGCT| C XX Csac_gene XhoI

11.5 HisPrep^{tm} FF 16/10 nickel column

Fused to the protein is a Histidine tag. This tag has an high affinity for Nickel ions, Figure 11-7. The nickel column consist of 90-µm beads of highly cross-linked agarose, to which a chelating ligand has been immobilized. This chelating ligand is charged with Ni^{2+} ions. Using a increasing salt gradient the bound protein can be recovered from the column

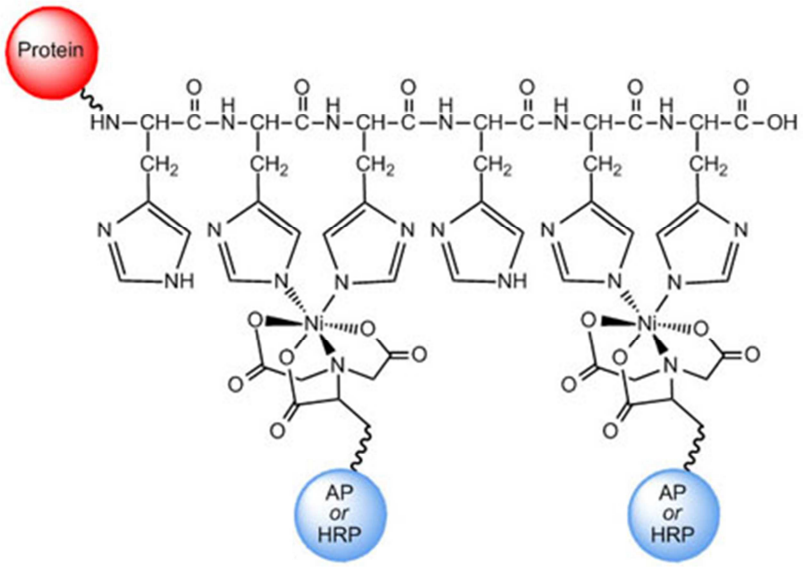

Figure 11-7 Display of interaction between HIS-tag and nickel ion fused to immobilized beads, shown as blue balls.

TECHNICAL SPECIFICATIONS HisPrep^{tm} FF 16/10

Medium	Ni Sepharose 6 Fast Flow
Column volume	1 ml and 5 ml
Dynamic binding capacity*	Approx. 40 mg histidine-tagged protein/ml medium
Column dimensions	0.7 × 2.5 cm (1 ml) 1.6 × 2.5 cm (5 ml)
Recommended flow rate†	1 ml/min (1 ml) 5 ml/min (5 ml)
Max. pressure†	3 bar (0.3 MPa, 42 psi)
pH stability‡	
Compatibility	Stable in all commonly used buffers, reducing agents, denaturants, and detergents, see Introduction to Tagged Protein Purification for more information.
Chemical stability	For information, see Ni Sepharose™ High Performance - High-performance Purification.
Storage	20% ethanol
Storage temperature	4°C to 30°C

** Protein binding capacity is protein-to-protein dependent*
† H_2O at room temperature
‡ Ni^{2+}-stripped medium

11.6 Size exclusion, desalting and superdex

Basically, a desalting column is a size exclusion column, figure 11.15. Pores of different sizes are present on the beads which are packed on the column. When a mixture of molecules passes the column, molecules smaller than the pore size can enter the pores whereas molecules larger than the pores cannot. Smaller molecules thus have more potential volume to pass before they have passed the column. Since a fixed flow rate is applied to the column, larger molecules are eluted earlier compared to smaller molecules.
The size of the pores on the beads determine the exclusion range. Thus it is possible to separate proteins form salt (desalting column), or large proteins from small ones (superdex column).

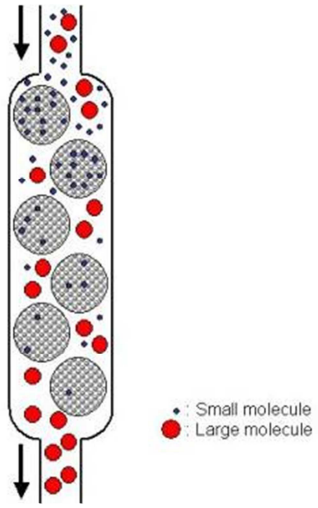

Figure 11-8 principle of a size exclusion column. Smaller molecules fit in the pores of the beads. Therefore, small molecules experience a larger volume in comparison to the larger molecules who can only fit in between the beads. This difference in relative volume results in different elution times.

11.6.1 Superdex™ 75 / Superdex™ 200 Columns

TECHNICAL SPECIFICATIONS

Superdex™

Exclusion limit (M_r)	
Superdex™ 75	1×10^5 globular protein
Superdex™ 200	1.3×10^6 globular protein
Separation range (M_r)	
Superdex™ 75	3000-70 000 globular protein
Superdex™ 200	10 000-600 000 globular protein
Matrix	Spherical composite of cross-linked agarose and dextran
Average particle size	13 µm
Chemical stability	Stable in all common buffers: 1 M acetic acid, 8 M urea, 6 M guanidine hydrochloride, 30% isopropanol, 70% ethanol, 1 M NaOH (for cleaning in place)
pH stability	3-12 (working and long term), 1-14 (short term)

Superdex™ 10/300 GL Columns (Tricorn)*

Bed dimensions	10 × 300 mm
Recommended sample volume	25□250 µl
Bed volume	24 ml
Max. pressure	
Superdex™ 75	18 bar (261 psi, 1.8 MPa)
Superdex™ 200	15 bar (217 psi, 1.5 MPa)
Max. flow rate (H_2O at 25°C)	
Superdex™ 75	1.5 ml/min
Superdex™ 200	1.0 ml/min
Theoretical plates	> 30 000 m^{-1}

* Columns are not suitable for use with ÄKTAprime™ plus system.

11.6.2 HiPrep™ 26/10 Desalting Columns

TECHNICAL SPECIFICATIONS

HiPrep™ 26/10 Desalting Column

Column volume	53 ml
Medium	Sephadex™ G-25 Fine
Column dimensions	2.6 × 10 cm
Void volume	15 ml
Sample volume	2.5-15 ml
Elution volume	7.5-20 ml
Exclusion limit (M_r)	5×10^3 globular protein
Max. flow rate (H_2O at 25°C)	450 cm/h (40 ml/min)
Recommended flow rate	100-300 cm/h (9-31 ml/min)
Max. pressure over the packed bed during operation	1.5 bar (22 psi, 0.15 MPa)
Column hardware pressure limit	5 bar (73 psi, 0.5 MPa)
Chemical stability	Stable in all commonly used buffer systems
pH stability	2-13 (long and short term)
Storage	20% ethanol
Storage temperature	4°C to 30°C

11.7Desalting chromatogram

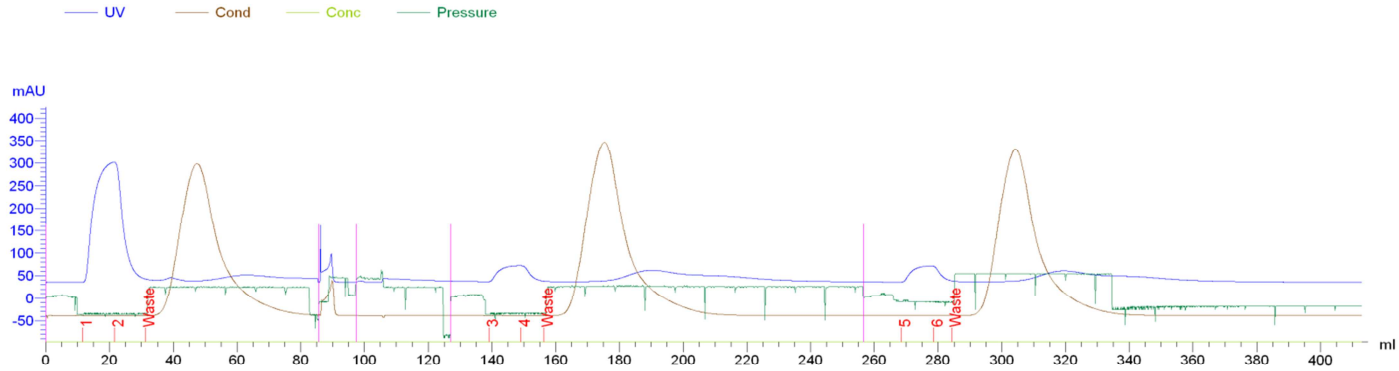

Figure 11-9 Desalting of PPDK, fraction 1 and 2, and PPi PFK fraction 4-6. The blue line represents the absorption, which is mainly caused by protein, the brown line is the conductivity. The green line is the pressure and the pink lines represent the injection points.

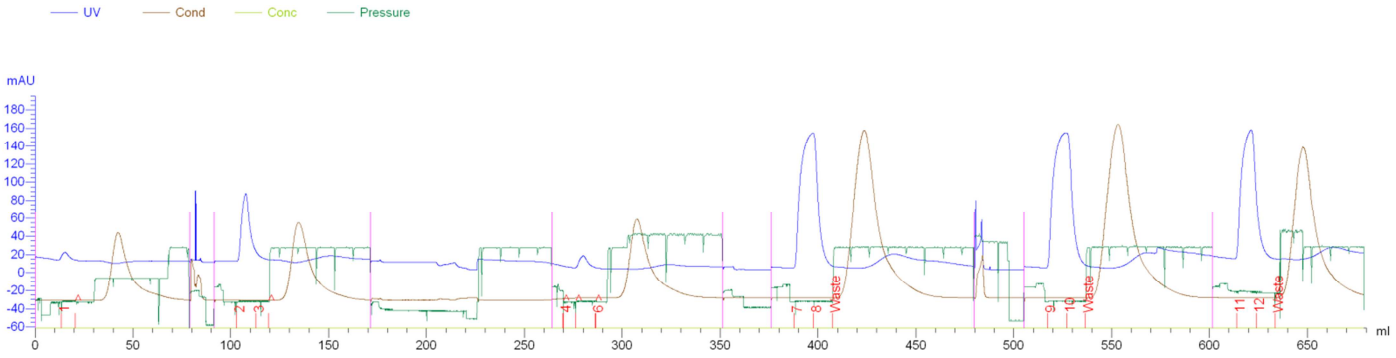

Figure 11-10 desalting of ATP PFK, fraction 1-3 and 5, and PK sample, 6-12. The blue line represents the absorption, which is mainly caused by protein, the brown line is the conductivity. Green is the pressure and the pink lines represent the injection points.

Table 11-1 Overview of desalting fractions and original sample

Fraction	**1**	**2**	**3**	**4**	**5**	**6**
Figure 11.10	ATP PFK nickel fraction 17	ATP PFK nickel fraction 18	ATP PFK nickel fraction 18		ATP PFK nickel fraction 19	PK pooled Ni fractions (16-23)
Figure 11.9	PPDK pooled Ni fractions (19-21)	PPDK pooled Ni fractions (19-21)	PPi PFK pooled Ni fractions (20-25)	PPi PFK pooled Ni fractions (20-25)	PPi PFK pooled Ni fractions (20-25)	PPi PFK pooled Ni fractions (20-25)
Fraction	**7**	**8**	**9**	**10**	**11**	**12**
Figure 11.10	PK pooled Ni fractions (16-23)	PK pooled Ni fractions (16-23)	PK pooled Ni fractions (16-23)	PK pooled fractions (16-23)	PK pooled Ni fractions (16-23)	PK pooled Ni fractions (16-23)

11.8 Calibration of superdex column

Figure 11-11, Figure 11-12 and Figure 11-13 show the calibration of the Superdex column.

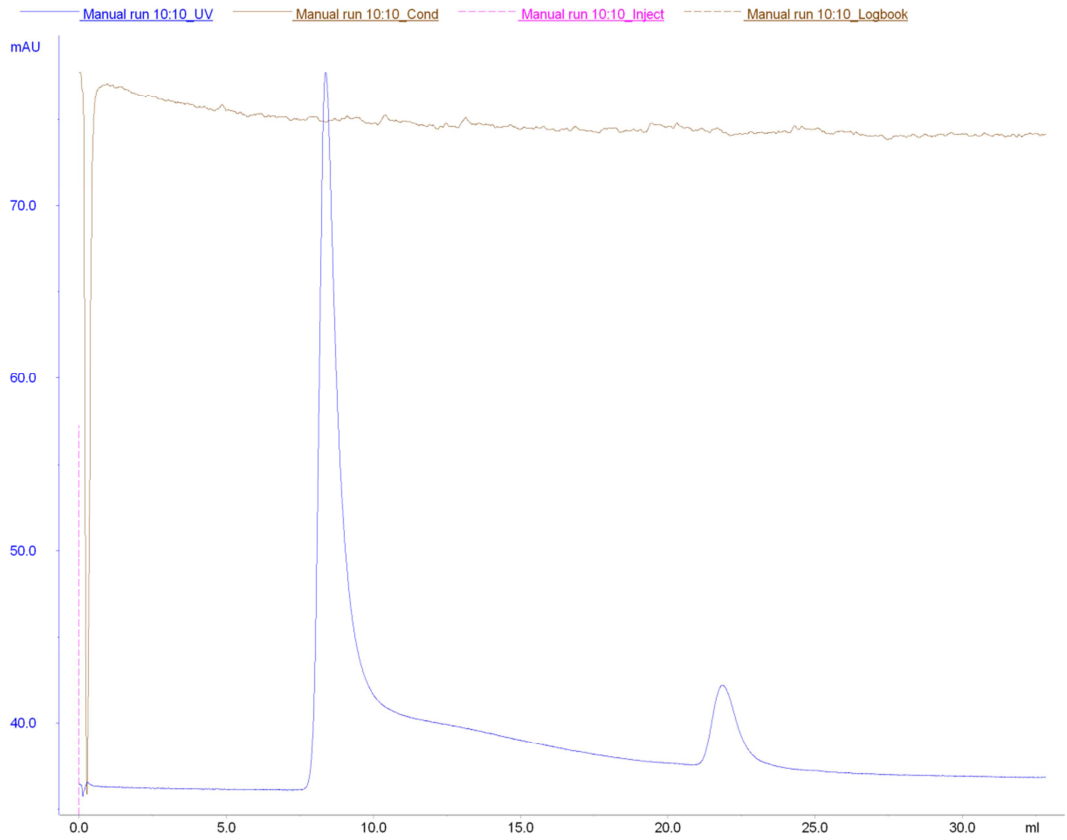

Figure 11-11 Superdex Blue Dextran, used to determine the void (Vo) volume

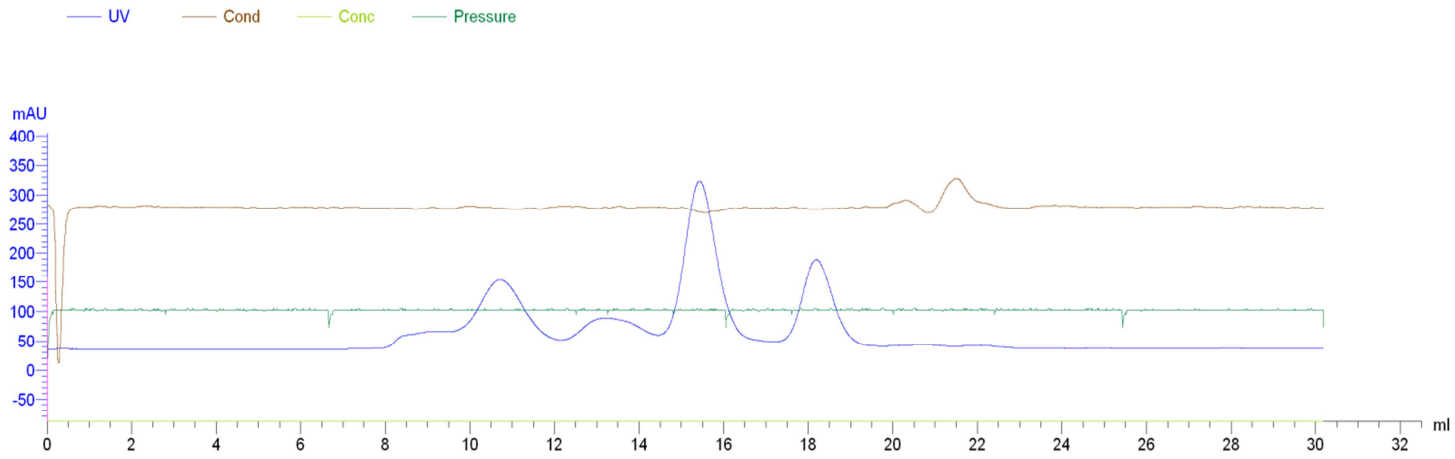

Figure 11-12 Run I superdex calibration, first part of calibration proteins. From left to right, Ferritin (440.00 kDa), Aldolase (158.000 kDa), Ovalbumin (43.000) and Ribonuclease A (13.700 kDa).

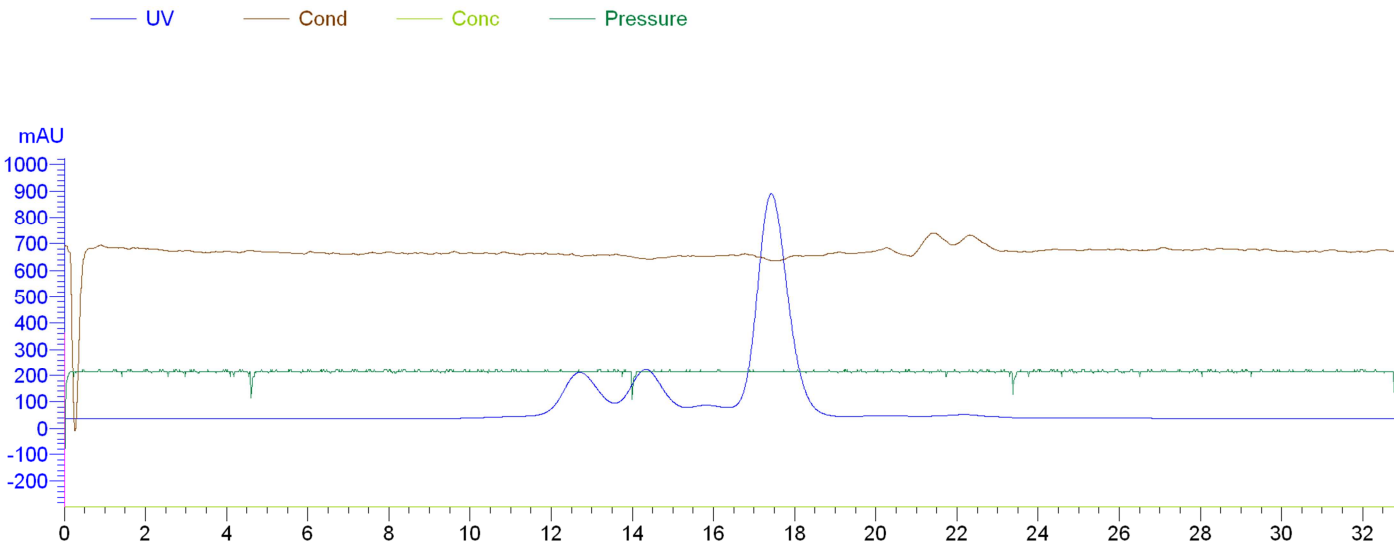

Figure 11-13 Run II superdex calibration, second mixture of calibration proteins, From left to right, Catalase (232.000 kDa) Albumin (67.000 kDa) and Chymotrypsinogen A (25.000 kDa).

11.9 Proteins on superdex

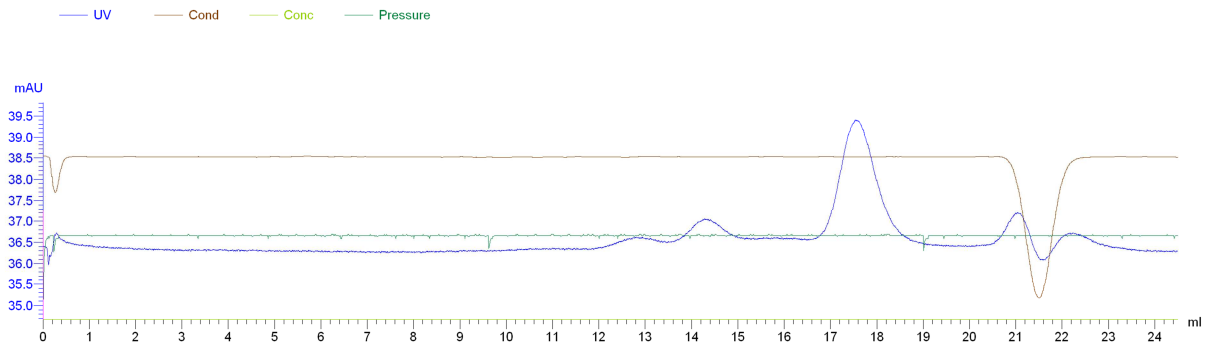

Figure 11-14 Superdex analysis of the ATP PFK. The blue line indicates protein fractions whereas the brown line indicated the conductivity, salt.

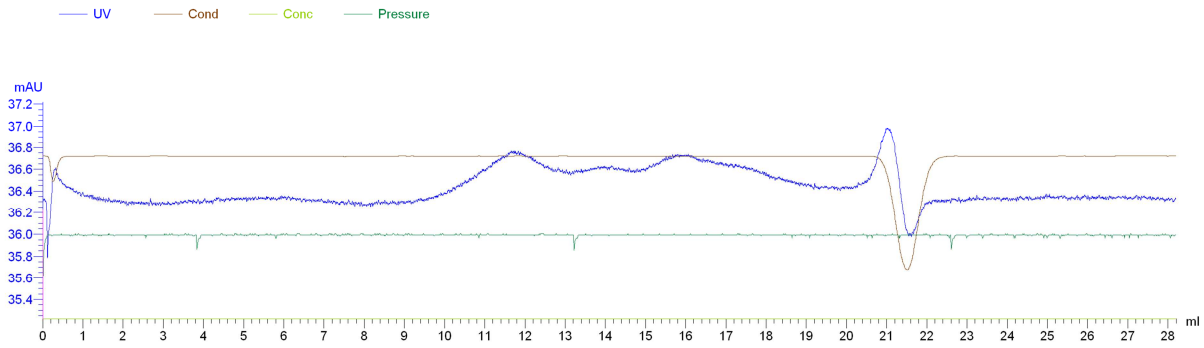

Figure 11-15 Superdex analysis of the PK. The blue line indicates protein fractions whereas the brown line indicated the conductivity, salt.

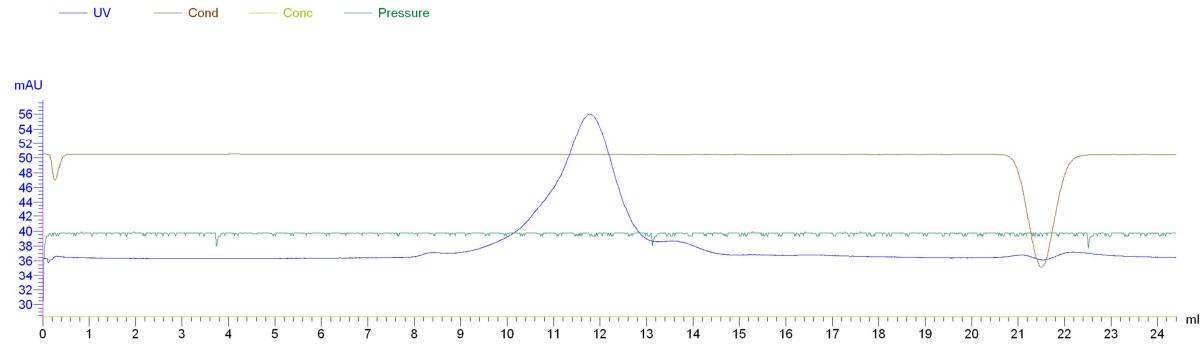

Figure 11-16 Superdex analysis of the PPDK. The blue line indicates protein fractions whereas the brown line indicated the conductivity, salt.

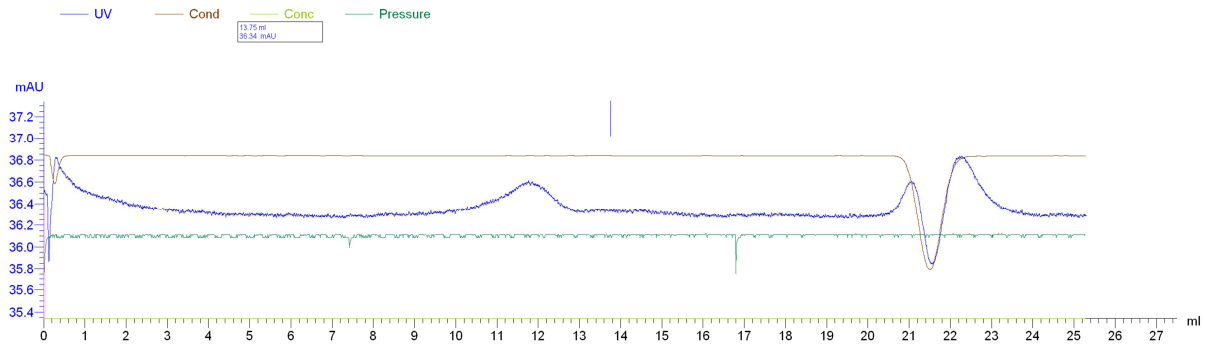

Figure 11-17 Superdex analysis of the PPi PFK. The blue line indicates protein fractions whereas the brown line indicated the conductivity, salt.

11.10Roti-Nanoquant measurement

Table 11-2 shows the calibration of the total protein determination. Table 11-3 displays the results from the total protein determination. Steps recalculating the direct result are shown in the table 11.3.

Table 11-2 Calibration curve using a BSA concentration series. The values from 590 nm and 450 nm are averaged of a duplo measurement. The standard deviation is also given. The 590/450 quotient is plotted against the concentration (not shown)

µg/ml protein	0	1	10	20	40
590 nm	0.391	0.386	0.458	0.590	0.756
st dev	0.000	0.004	0.004	0.018	0.005
450 nm	0.793	0.780	0.747	0.713	0.653
st dev	0.000	0.000	0.013	0.003	0.001
590/450	0.493	0.494	0.613	0.827	1.157

Table 11-3 Results from Roti-Nanoquant total protein determination. The numbers 1:20 and 1:40 indicate the dilution, 450 and 590 refers to the wavelength. The average concentration gives the corrected and averaged values from the diluted samples. Also the standard deviation and the variation quotient are given.

	450		590		actual µg/ml		Average	St dev	Vc %
	1:20	1:40	1:20	1:40	1:20	1:40	µg/ml		
PK	0.705	0.705	0.492	0.432	261.1	322.0	291.6	43.1	14.8
PPDK	0.658	0.714	0.557	0.469	436.0	425.8	430.9	7.2	1.7
ATP PFK	0.732	0.731	0.411	0.389	100.7	132.3	116.5	22.4	19.2
PPI PFK	0.734	0.740	0.415	0.378	105.3	82.1	93.7	16.4	17.5

11.11 Background on techniques and additional protocols

11.11.1 Preparation of Electro competent cells

Electro competent cells were used for plasmid transformations. DH5α was taken from the -80°C stock and plated on a normal LB agar plate. The plate was incubated overnight at 37°C in an incubation oven. A single colony was picked and inoculated in 3 ml of LB. The culture was incubated in a water bath (New Brunswick) at 37°C overnight.
1 ml of culture was transferred to 500 ml LB and incubated at 37°C until an Optical Density (OD) at 600 nm of 0,6-0,9 was reached. The cells were harvested by centrifugation using a sorvall RC6 at 4ºC, 4500 min^{-1} for 10 min. The pellet was washed with sterile cold MilliQ and twice with sterile cold 10% glycerol in MilliQ. The washed pellet was resuspended in 1-3 ml of sterile cold 10% glycerol in MilliQ and distributed in aliquots of 50 µl in eppendorf tubes. These electro competent cells were stored at -80°C.

11.11.2 Electro transformation

For transformation 50 µl of electro competent DH5α cells were mixed with 2 µl of plasmid solution and placed in a transformation cuvette of 2 mm. Using the electro cell manipulator ECM 630 Precision Pulse to deliver a pulse of 2500 V during 5-6 msec. After the pulse the cells were resuspended in 950 µl of SOC medium (Maniatis) and incubated for 45-60 min at 37°C in a water bath. Subsequently, the cells were spun down for 1 minute at 13.000 rpm in a eppendorf table centrifuge and resuspended in 100 µl SOC medium. This culture was plated on a LB kanamycin (50 µl/ml) selection plate and incubated overnight in a 37°C incubation stove.

11.11.3 Induction of protein production

The gene is placed behind a T7 promotor on the pET24d plasmid. The production strain used, BL21 contains DE3 (therefore BL21de3), a λ prophage carrying the T7 RNA polymerase gene (OpenWetWare 2011). The T7 RNA polymerase gene is normally repressed by LacI. However this repression can be relieved by addition of IPTG. Thus protein production is indirectly induced by IPTG, see Figure 11-18

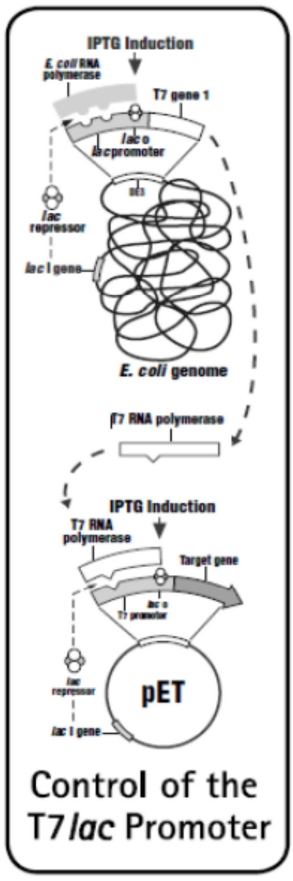

Figure 11-18 Method of protein production using a BL21de3 production strain, a pET24d vector and IPTG induction. Picture taken from (Novagen 2011).

11.11.4 Heat treatment

Since the proteins of interest are heat stable, a heat treatment step might be very efficient in removing cellular E.coli proteins. To none heat stable proteins, heat treatment will give the same effect as boiling an egg. The proteins will denature and precipitate. By centrifugation the precipitated none heat stable proteins can be separated from the still soluble heat stable proteins.

11.11.5 SDS-page

SDS-PAGE, **s**odium **d**odecyl **s**ulfate **p**oly**a**crylamide **g**el **e**lectrophoresis in full, is a protein separation technique where the proteins are compared solely on their size. This was achieved because SDS (Figure 11-19) can bind to the protein and disrupt the conformation due to negative charge on the SDS. Negative charge from the SDS is significantly greater than the authentic charge of the protein. Therefore the protein forms a rod like shape and since the charge per mass is the same for all proteins, separation based on size is now possible. The proteins are loaded on a gel and a charge is applied, causing the proteins to migrate through the gel according to size, Figure 11-20.

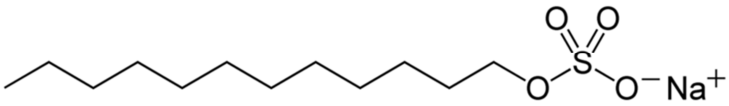

Figure 11-19 sodium dodecyl sulfate, the 12 carbon tail in combination with the sulfate group give this molecule detergents like properties.

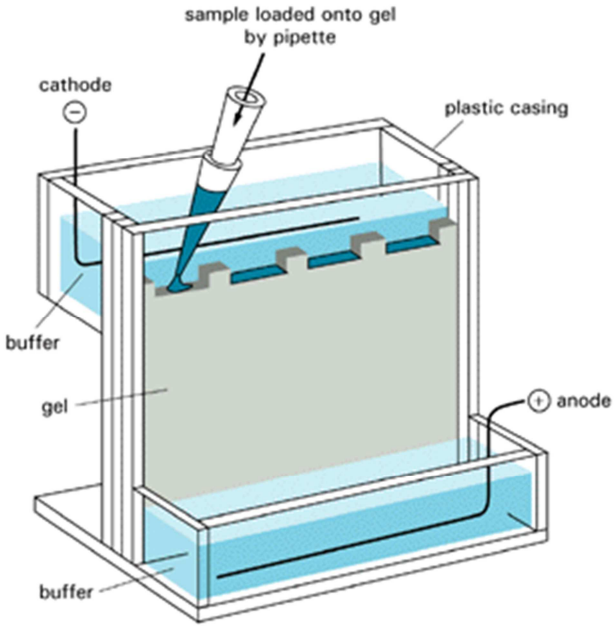

Figure 11-20 SDS-page electrophoreses set-up. The protein samples are loaded on the gel, due to the SDS the proteins are negatively charged and therefore migrate towards the anode.